ELSEVIER

Coordination Chemistry Reviews 143 (1995)
297–330

COORDINATION CHEMISTRY REVIEWS

Transition metal boride clusters at the molecular level

Catherine E. Housecroft

Institut für Anorganische Chemie, Spitalstrasse 51, CH-4056 Basel, Switzerland

Received 12 August 1994; revised 7 October 1994

Contents

Abstract

Low oxidation state transition metal clusters which contain one or two boron atoms in fully or semi-interstitial sites are reviewed. In such environments, the boron atom does not bear a terminal hydrogen atom. This area of research has been developed primarily over the last decade, and now includes a range of homo- and heterometallic systems. Metal frameworks that are represented include the M_4 butterfly, the M_5 square-based pyramid, the M_6 octahedron and the M_6 trigonal prism, together with a variety of more unusual geometries. Synthetic and structural studies form the basis of the review. Chemical reactivity patterns of the butterfly

SSDI 0010-8545(94)07007-5

clusters (which support semi-interstitial boron atoms) are discussed in detail; reactions include B—C and B—N couplings at the semi-interstitial atom as well as metal framework expansion which transforms the boron atom from semi- to fully interstitial.

Keywords: Transition metal clusters; Boron; Reactivity

List of Abbreviations

Cp	η^5-C_5H_5
Cp*	η^5-C_5Me_5
dppf	1,1′-bis(diphenylphosphino)ferrocene
PPN^+	$(Ph_3P)_2N^+$
EAN	effective atomic number

1. Introduction

Over the past decade, several reviews have illustrated that the area of metal-rich metallaboranes is rapidly expanding [1–7]. The area is quite distinct from that of the larger boron cage (boron-rich) metallaboranes [8–10]. The characteristic feature that separates the boride clusters from the metallaboranes is the greater number of boron-to-metal bonding contacts in the former species; this is at the expense of boron–hydrogen bonds. This difference necessarily generates a quite different type of environment for the boron atom and leads, not surprisingly, to some quite novel chemistry. A true boride cluster contains a "naked" boron atom, one which is denuded of hydrogen atoms.

The compounds that we shall deal with in this review have transition metal carbonyl frameworks or may incorporate transition metal cyclopentadienyl units. In each case, the metal skeleton encapsulates or partially encapsulates one or two boron atoms. Another group of boron-containing species possesses hexametal halide cores and includes compounds of the type $MM'[Zr_6Cl_{15}B]$ ($M = M'$ or $M \neq M'$; M and M′ = alkali metals) [11,12]. These represent an altogether different type of cluster system from the low oxidation state metal carbonyl clusters and, for this reason, are not included here.

Transition metal carbonyl clusters which contain interstitial carbon or nitrogen atoms have been documented in the literature for some time [6,13–16]. Typical cavities in which a carbon or nitrogen atom might be accommodated are the octahedron and trigonal prism (Fig. 1). Examples include $[Co_6(CO)_{13}C]^{2-}$ [17], $[Rh_6(CO)_{15}C]^{2-}$ [18], $[Co_6(CO)_{13}N]^-$ [19] and $[Co_6(CO)_{15}N]^-$ [20]. On moving to the second (or lower) row of the periodic table, atoms of the p block elements necessarily require larger cavities in which to be accommodated. The octahedral site is not now observed, but the trigonal prismatic cavity is large enough to accommodate, for example, a phosphorus atom as in $[Os_6(CO)_{18}P]^-$ [21]. The size of the metal atom (which naturally influences the size of the cavity) is a critical factor. The larger main group atoms can also aid in the stabilization of metal cages

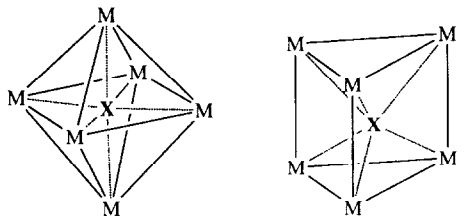

(a) (b)

Fig. 1. (a) Octahedral and (b) trigonal prismatic M_6 cages encapsulating an atom X (e.g. X=C or N).

not seen for the first row interstitial atoms; examples are $[Rh_9(CO)_{21}P]^{2-}$ [22], $[Rh_{10}(CO)_{22}As]^{3-}$ [23] and $[Rh_{12}(CO)_{27}Sb]^{3-}$ [24].

Let us return to the first row of the p block, and specifically to carbon and nitrogen. The fully interstitial atom is complemented by a range of compounds which exhibit a C or an N atom in a semi-interstitial or an exposed site. The common range of metal skeletons is shown in Fig. 2; note that each M_x cage is a fragment of an octahedron. A rich chemistry has been developed for the M_4C framework. One of the most beautiful examples comes from the work of Shriver and his group; they have demonstrated the reduction of a cluster-bound CO ligand to CH_4, the key atom in the sequence being the semi-interstitial carbon atom supported in a butterfly framework of iron atoms [25–27].

When studies of the formation and reactivity of discrete molecular boride clusters with metal carbonyl skeletons first emerged, it was of interest to see to what extent the compounds would mimic their carbide and/or nitride counterparts. The periodic relationship between B, C and N means that, for a cluster with a given electron count (see, for example, Ref. [28]), a series of isoelectronic boride, carbide and nitride clusters cannot be exactly comparable. This is amply demonstrated in the series of butterfly clusters $[Ru_4(CO)_{12}N]^-$ [29], $[HRu_4(CO)_{12}CH]$ [30], and $[HRu_4(CO)_{12}BH_2]$ [31,32] where the additional requirement of hydrogen atoms in the carbide and boride cases can be seen.

In addition to being looked at in a comparative sense, transition metal boride

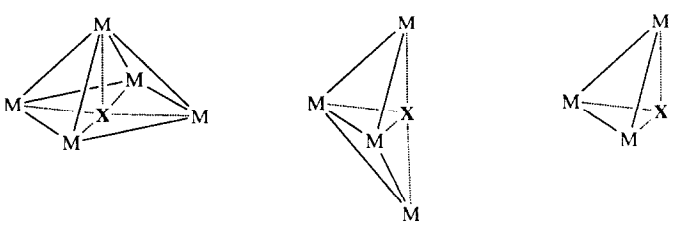

(a) (b) (c)

Fig. 2. Semi-interstitial and exposed sites for an atom of a p block element X: (a) a square-based pyramidal framework; (b) a butterfly framework; (c) a metal triangle.

clusters constitute a group of compounds that is worthy of study in its own right. The unusual bonding abilities of a boron atom are well established in elemental boron and the boron hydrides, and placing this atom in yet another type of environment in which multicentre bonding is required provides another avenue of new chemistry to explore. The link to the solid state [4,33] is also important. The structural motifs which will be discussed in this review sometimes parallel those found in bulk state metal borides. An example is the trigonal prismatic geometry (Fig. 1(b), X=B) of the core of $[H_2Ru_6(CO)_{18}B]^-$ [34,35] which replicates a structural unit observed in Ru_7B_3 [33]. Work of Fehlner and co-workers has shown that thin films of metal borides can be produced, for example via the pyrolysis of the cluster $[HFe_4(CO)_{12}BH_2]$ with the Fe:B stoichiometry remaining 4:1 [36]. In contrast, boron-rich borides (e.g. YbB_4 and EuB_6) may be prepared from borohydride complexes [37].

This review concentrates on clusters with fully or semi-interstitial boron atoms. Clusters in which the boron atom bears a terminal hydrogen atom have been excluded from the discussion. The M_3X (X=B) skeleton depicted in Fig. 2(c) will be represented only in discussions of synthesis where this unit is used as a basic building block for attaining higher nuclearity clusters. Some of the chemistry of these M_3B systems has previously been reviewed [1,2,5,7].

2. ^{11}B nuclear magnetic resonance spectroscopy

The role of ^{11}B nuclear magnetic resonance (NMR) spectroscopy in the characterization of boron-containing clusters is vitally important. Previously, it had been noted that the chemical shift values for ^{13}C [13] and ^{15}N [16] NMR spectral resonances were sensitive to environment, with interstitial atoms being characterized by unusually low field chemical shifts. This same phenomenon has been observed in the ^{31}P NMR spectra of phosphide clusters. Trends in chemical shift values for interstitial atoms have been addressed independently by several groups. Correlations have been observed between chemical shift values (^{11}B, ^{13}C and ^{15}N) and the compression of the cluster cavity [38]. Larger deshielding is experienced by a carbon or nitrogen atom situated in the cavity in an M_6 octahedron than in an M_6 trigonal prism [38,39] but, for boron, the deshielding is about the same in the two environments [34]. Nuclear deshielding is approximately the same for B, C and N in an octahedral cavity but, when encapsulated in a trigonal prismatic cage, the nuclei experience deshielding in the order B>C>N. In octahedral cages, the net M—X interaction has been shown to be similar for X=B or C [40].

While chemical shift values for interstitial atoms are particularly characteristic (the signals are usually sharp as well as being at low field) it has also been observed that the shift value is dependent on the number of metal-to-boron direct interactions even when the boron nucleus is not inside a metal cavity. A parametrized model has been developed using available data for ferraborane clusters to allow new $\delta(^{11}B)$ values to be predicted [41]. In our own work, we have observed that a similar parametrization can be developed to deal with Ru—B bonds [42]; as with the

Table 1
Selected ^{11}B nuclear magnetic resonance shifts illustrating the range of values for fully and semi-interstitial boron nuclei in cages of group 8 metal atoms: the cavity size and connectivity of the boron atom are indicated

Compound	Cavity	Connectivity of of boron atom[a]	δ (^{11}B)[b]	Refs.
$[HFe_4(CO)_{12}BH_2]$	Fe_4 butterfly	4	+116	[44][c]
$[HFeRu_3(CO)_{12}BH_2]$	$FeRu_3$ butterfly	4	+114	[45]
$[HRu_4(CO)_{12}BH_2]$	Ru_4 butterfly	4	+109.9	[31,32]
$[HOs_4(CO)_{12}BH_2]$	Os_4 butterfly	4	+119.7	[46]
$[HOs_5(CO)_{16}B]$	Os_5 bridged butterfly	5	+184.4	[46]
$[HRu_6(CO)_{17}B]$	Ru_6 octahedron	6	+193.8	[47]
$[Ru_6(CO)_{17}B][PPN]$	Ru_6 octahedron	6	+196	[47]
$[Ru_6(CO)_{17}B][HNMe_3]$	Ru_6 octahedron	6	+202.2	[48]
$[H_2Ru_6(CO)_{18}B][PPN]$	Ru_6 trigonal prism	6	+205.9	[34,35]

[a] Strictly, we should include a detailed breakdown into M−B, M−H−B etc. (see Ref. [41]).
[b] Referenced with respect to $BF_3{\cdot}OEt_2$; downfield shifts are positive. Some signals are solvent dependent (see individual reference).
[c] This shift was originally reported as +106 but see, for example, Refs. [5] and [41].

ferraboranes, fits between experimental and calculated values for the ruthenaboranes and borides are good and allow an early (if very approximate) structural assignment to be made. In addition, ^{11}B NMR chemical shifts have been correlated with boron Mulliken populations calculated using the Fenske–Hall quantum chemical method. The large deshielding caused by Fe–B interactions can be attributed to an increase in the multiple bond contributions to the shielding tensor [41].

Further work by Fehlner et al. has involved the use of the Fenske–Hall technique to illustrate that the sign and magnitude of the paramagnetic contribution to the shielding correlate well with observed values of ^{11}B NMR chemical shifts [43].

Table 1 gives representative values of ^{11}B NMR spectral shifts for group 8 metal containing boride clusters.

3. Clusters with a butterfly framework containing semi-interstitial boron atoms

3.1. Synthesis

The semi-interstitial atom is defined here as one which lies within an M_4 butterfly framework (Fig. 2(b)). The first such boride to be reported was $[HRu_4(CO)_{12}BH_2]$ (Fig. 3) [49]. It was prepared as a byproduct in the reduction of $Ru_3(CO)_{12}$ by $[BH_4]^-$ but, at this stage, characterization was tentative and two structures were proposed. In 1982, the iron analogue $[HFe_4(CO)_{12}BH_2]$ was prepared by the reaction of $[Fe_2(CO)_6B_2H_6]$ with $Fe_2(CO)_9$ [44]. This cluster expansion reaction was subsequently studied more extensively and an analogous reaction using the conjugate base of $[Fe_2(CO)_6B_2H_6]$ gives a route to $[HFe_4(CO)_{12}BH]^-$ [50]. In this case,

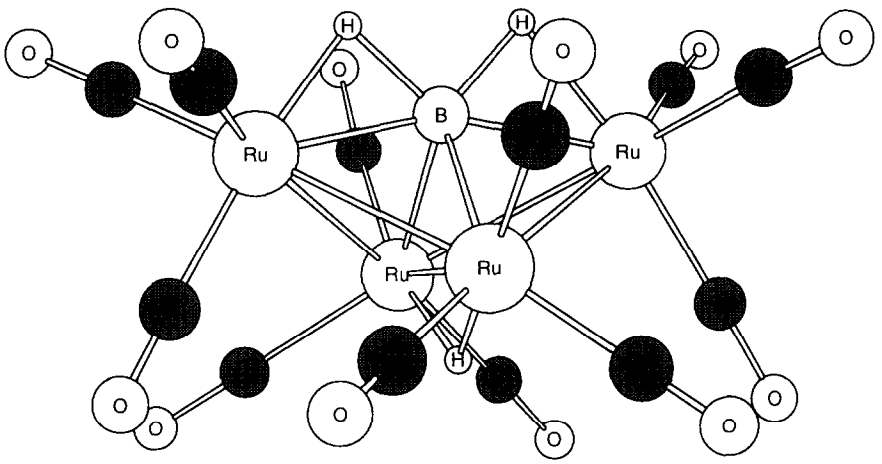

Fig. 3. The structure of $[HRu_4(CO)_{12}BH_2]$; both the iron and the osmium analogues have been fully characterized.

however, a reduced yield of the tetrairon cluster is obtained as $[Fe_3(CO)_{10}BH_2]^-$ becomes the dominant product. A further route to $[HFe_4(CO)_{12}BH_2]$ is through the aggregation of fragments in the reaction of $Fe_2(CO)_9$, $Fe(CO)_5$, BH_3·thf and $Li[BHEt_3]$; $[HFe_4(CO)_{12}BH_2]$ can be isolated as one of several cluster species after acidification [51]. Another method dependent on the aggregation of small fragments is the reaction of $Fe(CO)_3(\eta^2$-*cis*-cyclooctene) with BH_3·SMe_2 or BH_3·thf. With a ratio of Fe:B of 4:3, the pathway favours $[HFe_4(CO)_{12}BH_2]$ as the product although yields are low [52].

Three methods of preparing $[HRu_4(CO)_{12}BH_2]$ have been reported. The first [31] involves the reaction of $H_4Ru_4(CO)_{12}$ with BH_3·thf in dichloromethane at 40 °C for several days. The tetraruthenaborane is formed in 60% yield. A lower yield can be obtained (in a much shorter time period) by treating $Ru_3(CO)_{12}$ with BH_3·thf and $Li[BHEt_3]$ at ambient temperature followed by addition of acid [32]. More recently, it has been shown that photolysis of $[Ru_3(CO)_9BH_5]$ in dichloromethane (16 h) gives $[HRu_4(CO)_{12}BH_2]$ in 50% yield. This pathway is summarized in Fig. 4; the second product of the reaction is $[HRu_6(CO)_{17}B]$ (see Section 5) [45]. Use can be made of this type of assembly to introduce other metal fragments and generate heterometallic butterfly systems (see below).

The prototype for the $M_3B \rightarrow M_4B$ cluster expansion is seen in the reaction of $[Fe_3(CO)_9BH_4]^-$ with $Fe_2(CO)_9$ to yield the conjugate base of $[HFe_4(CO)_{12}BH_2]$ [51,53]. Quantitative reactions are unusual in cluster chemistry: degradation and reaggregation of fragments are commonplace. However, the formation of $[HFe_4(CO)_{12}BH]^-$ by this route is an exception and the reaction has been shown to follow the path

$$[Fe_3(CO)_9BH_4]^- + 2Fe_2(CO)_9 \rightarrow [HFe_4(CO)_{12}BH]^- + H_2 + 3Fe(CO)_5 \qquad (1)$$

A range of ruthenium-based clusters has been generated in reactions similar to

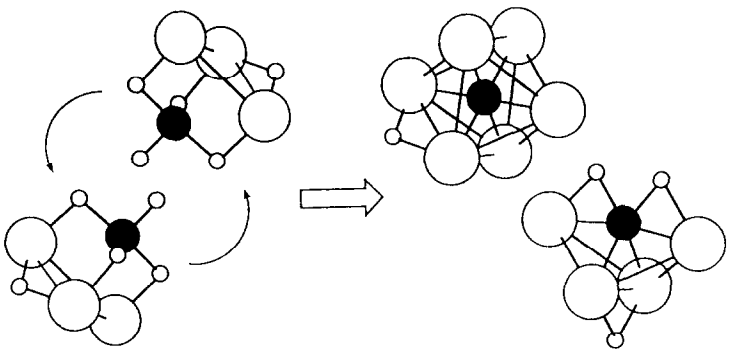

Fig. 4. Schematic representation of the assembly of $[HRu_4(CO)_{12}BH_2]$ and $[HRu_6(CO)_{17}B]$ from $[HRu_3(CO)_9BH_4]$.

that in Eq. (1). However, it has been found that a photolysis route involving neutral clusters provides a more effective means of synthesis, in part because of the relative ease of separating neutral (rather than anionic) cluster products by chromatography. Using this methodology, $[HFeRu_3(CO)_9BH_2]$ has been prepared from $[Ru_3(CO)_9BH_5]$ and $Fe(CO)_5$ [45], and the clusters $[H\{CpM(CO)_2\}Ru_3(CO)_9BH]$ (M = Mo or W) have been synthesized from $[Ru_3(CO)_9BH_5]$ and $[\{CpM(CO)_3\}_2]$ [54]. Interestingly, the reactions with the group 6 metal fragments exhibit competitive pathways: one in which the metal adds to the Ru_3B core and one in which the metal displaces the boron atom from the cluster.

Related to the previous assembly reactions is that of adding an electrophilic metal fragment to a cluster anion in order to achieve an $M_3B \rightarrow M_3M'B$ expansion. This general building-block approach is not new to cluster chemistry [55]. It works effectively in the reaction of $[Ru_3(CO)_9BH_4]^-$ with $[\{Cp^*RhCl_2\}_2]$ to yield the butterfly cluster $[H\{Cp^*Rh\}Ru_3(CO)_9BH_2]$ [56]. The $\{Cp^*Rh\}$ fragment is isolobal with $\{Ru(CO)_3\}$ and therefore $[H\{Cp^*Rh\}Ru_3(CO)_9BH_2]$ is directly related to $[HRu_4(CO)_9BH_2]$. However, products are not always as expected, and the same reaction strategy, repeated using iridium instead of rhodium, leads to $[H\{Cp^*Ir\}Ru_3(CO)_{10}BH_2]$ in place of the expected "$[H\{Cp^*Ir\}Ru_3(CO)_9BH_2]$". The additional carbonyl ligand provides two more electrons making the cluster a 64 electron system; the product therefore adopts an "opened butterfly" framework (Fig. 5) [56]. When the incoming electrophile is generated from $[\{Cp^*RuCl_2\}_n]$, then the product is again not that predicted. In this case an unusual "spiked butterfly" cluster $[H_2Ru_5(CO)_{13}Cp^*BH_2]$ is generated, the core structure of which is shown in Fig. 6 [57].

The isolation of $[H_2Ru_5(CO)_{13}Cp^*BH_2]$ [57] is an example of a product of expansion which exceeds the expected $M_3B \rightarrow M_3M'B$ sequence. It is not alone. The reaction of $[Ru_3(CO)_9BH_4]^-$ with the rhodium(I) dimer $[\{Rh(CO)_2Cl\}_2]$ leads to two clusters with fully interstitial atoms (see Section 5) [58].

The tetraosmium butterfly cluster $[HOs_4(CO)_{12}BH_2]$ was the last of these group 8 species to be reported. Over the past decade, Shore and coworkers have elegantly

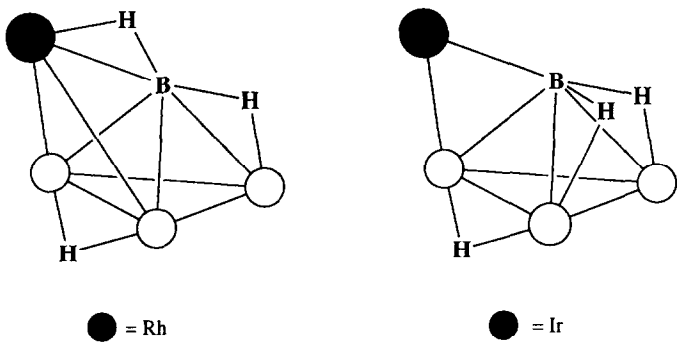

Fig. 5. A comparison of the core atom arrangements in $[H\{Cp^*Rh\}Ru_3(CO)_9BH_2]$ and $[H\{Cp^*Ir\}Ru_3(CO)_{10}BH_2]$. The former has 62 cluster electrons while the latter has 64.

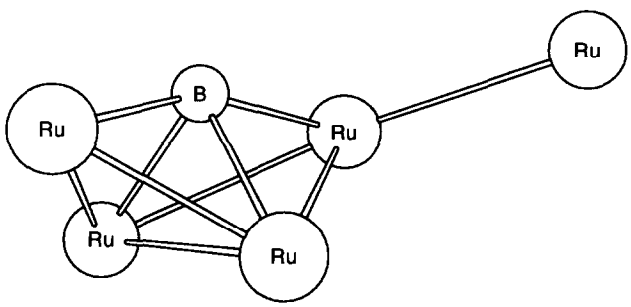

Fig. 6. The Ru_5B core of $[H_2Ru_5(CO)_{13}Cp^*BH_2]$.

demonstrated the diverse nature of the chemistry of $[H_3Os_3(CO)_9B(CO)]$, formed by the hydroboration of $[H_2Os_3(CO)_{10}]$ [7,59]. The thermolysis of $[H_3Os_3(CO)_9B(CO)]$ in toluene (110 °C, 6 days) leads to the formation of a mixture of $[HOs_4(CO)_{12}BH_2]$ (4.5% yield) and $[HOs_5(CO)_{16}B]$ (3.4% yield). The latter cluster is discussed further in Section 4 [46].

3.2. Structure

The three parent butterfly boride clusters $[HFe_4(CO)_{12}BH_2]$ [44,60], $[HRu_4(CO)_{12}BH_2]$ (Fig. 3) [31] and $[HOs_4(CO)_{12}BH_2]$ [46] have all been crystallographically characterized. Each exhibits the M_4 butterfly metal framework with the boron atom within bonding contact of all four metal atoms. Each metal atom carries three terminal carbonyl ligands. The "hinge" edge of the M_4 butterfly is bridged by a hydrogen atom, as are the two $M_{wingtip}-B$ edges. The core structure for $[HRu_4(CO)_{12}BH_2]$ is shown in Fig. 7.

Two parameters that are regularly used to define the nature of these and related butterfly clusters are the internal dihedral angle of the M_4 framework and the height of the boron atom above the $M_{wingtip}-M_{wingtip}$ axis (Table 2). Inspection of these geometrical parameters for $[HFe_4(CO)_{12}BH_2]$ together with the results of

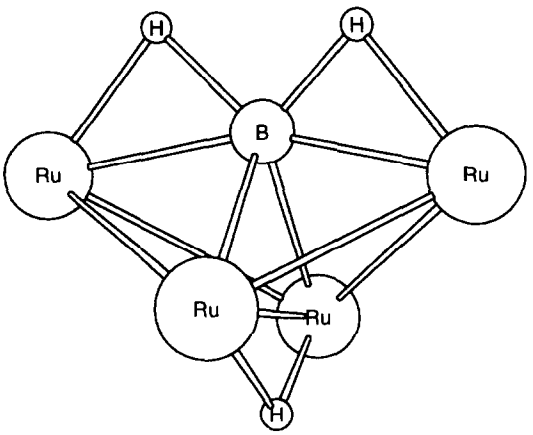

Fig. 7. The HRu_4BH_2 core of $[HRu_4(CO)_{12}BH_2]$; the Fe and Os analogues possess similar structural characteristics (see Table 2).

Table 2
Structural parameters that describe the M_4B framework in some butterfly clusters containing a semi-interstitial boron atom

Compound	Internal dihedral angle of the M_4 frame (deg)	Height of B atom above the $M_{wingtip}-M_{wingtip}$ axis (Å)	Ref.
$[HFe_4(CO)_{12}BH_2]$	114.0	0.31	[44,60]
$[HRu_4(CO)_{12}BH_2]$	118	0.39[a]	[31]
$[HOs_4(CO)_{12}BH_2]$	113	0.31[a]	[46]
$[H_2Ru_5(CO)_{13}Cp^*BH_2]$	114.2	0.31	[57]

[a] Calculated from atomic coordinates.

Fenske–Hall molecular orbital calculations support a bonding description of these clusters as *arachno* [61] species; this is consistent with the boron atom contributing all three of its valence electrons to cluster bonding. In terms of the EAN approach, each of $[HFe_4(CO)_{12}BH_2]$, $[HRu_4(CO)_{12}BH_2]$ and $[HOs_4(CO)_{12}BH_2]$ is counted as a 62 electron cluster [62,63], again with the boron atom acting as a three electron contributor.

The structure of $[H_2Ru_5(CO)_{13}Cp^*BH_2]$ [57] is closely related to that of $[HRu_4(CO)_{12}BH_2]$. The terminal carbonyl ligands associated with the wingtip ruthenium atoms in $[HRu_4(CO)_{12}BH_2]$ (Fig. 3) are arranged so that two occupy equatorial sites and one is axial i.e. the axial ligand is trans to a B—H—Ru bridging hydrogen atom) [31]. In $[H_2Ru_5(CO)_{13}Cp^*BH_2]$, one equatorial wingtip terminal carbonyl ligand is replaced by an $\{RuCp^*(CO)_2\}$ spike (Fig. 6); the $Ru_{wing}-Ru_{spike}$ edge is bridged (see below) by a hydrogen atom. The $Ru_{wing}-Ru_{spike}$ bond distance is 3.115(1) Å which is longer than the average intrabutterfly Ru—Ru edges (average

2.865(1) Å. For the butterfly unit to retain its 62 electron count, the $\{HRuCp^*(CO)_2\}$ unit needs to provide two electrons to the cluster. The spike ruthenium atom may be considered to be a localized 18 electron centre. This in turn means that the $Ru_{wing}-Ru_{spike}$ bond should be considered to be a localized two-centre two-electron bond. The hydrogen atom associated with this edge may well then be considered as being terminal with respect to the butterfly framework rather than truly bridging the $Ru_{wing}-Ru_{spike}$ edge. Such an ambiguity must remain: estimated standard deviations the on these Ru—H distances are too large to permit a definite solution to the problem (Ru—H distances, 1.71(7) Å and 1.69(7) Å).

The heterometallic butterfly $[H\{Cp^*Rh\}Ru_3(CO)_9BH_2]$ exhibits a core that is similar to that observed for the family of clusters described above. The geometry has been crystallographically confirmed for the phosphine derivative $[H_2\{Cp^*Rh\}Ru_3(CO)_8(PPh_3)BH]$ although the substitution of a PPh_3 for a CO ligand results in a migration of one Ru—H—B bridging hydrogen atom to an Ru—H—Ru site [56]. The changes in cluster hydrogen positions are apparent in differences recorded in the ^1H NMR spectra of the two compounds. The rhodium atom in $[H_2\{Cp^*Rh\}Ru_3(CO)_8(PPh_3)BH]$ (and, by inference, in $[H\{Cp^*Rh\}Ru_3(CO)_9BH_2]$) resides in a wingtip site and this illustrates that the tetrahedral $\{Ru_3B\}$ unit of the precursor $[Ru_3(CO)_9BH_4]^-$ (see Section 3.1) remains intact during cluster expansion.

Two further heterometallic clusters exhibiting semi-interstitial boron atoms are $[H\{CpMo(CO)_2\}Ru_3(CO)_9BH]$ and $[H\{CpW(CO)_2\}Ru_3(CO)_9BH]$ (Fig. 8) and the latter has been structurally characterized [54]. The $\{CpW(CO)_2\}$ unit occupies a wingtip site in the M_3M' butterfly framework. The $\{CpMo(CO)_2\}$ and $\{CpW(CO)_2\}$ fragments each supply one more electron to the cluster than the $\{M(CO)_3\}$ (M = Fe, Ru or Os) or $\{Cp^*Rh\}$ units discussed above. The cluster responds accordingly by possessing just two hydrogen atoms rather than three as in the compounds discussed earlier. Spectroscopic data support the positioning of the two hydrogen atoms along the $Ru_{hinge}-Ru_{hinge}$ and $Ru_{wingtip}-B$ edges. The presence of only one boron-bound hydrogen atom is evident in the proton-coupled ^{11}B NMR spectrum which is a doublet ($J_{BH} \approx 65$ Hz) in both the compounds $[H\{CpMo(CO)_2\}Ru_3(CO)_9BH]$ and $[H\{CpW(CO)_2\}Ru_3(CO)_9BH]$.

The series of clusters described in this section illustrates how the environment of the boron atom can be tuned by varying the metal or ligand shell while maintaining the same overall $M_{4-x}M_xB$ core. Two methods are exemplified: (i) varying the number of electrons available from the metal fragments for cluster bonding or (ii) altering the *exo* ligands. In the compounds $[HFe_4(CO)_{12}BH_2]$, $[HRu_4(CO)_{12}BH_2]$, $[HOs_4(CO)_{12}BH_2]$, $[H\{Cp^*Rh\}Ru_3(CO)_9BH_2]$ and $[H_2Ru_5(CO)_{13}Cp^*BH_2]$, each metal fragment in the butterfly framework supplies 14 electrons by the EAN approach [62,63] (or two electrons by Wade's approach [61]). The boron atom uses three electrons and to make up the 62 electron count of the M_4- butterfly, three H atoms are needed. The boron atom resides in a semi-interstitial site but is still associated with two (non-terminal) hydrogen atoms. The environment can be shifted in favour of a more "boridic" environment i.e. fewer B—H interactions and more direct B—M interactions) by exchanging

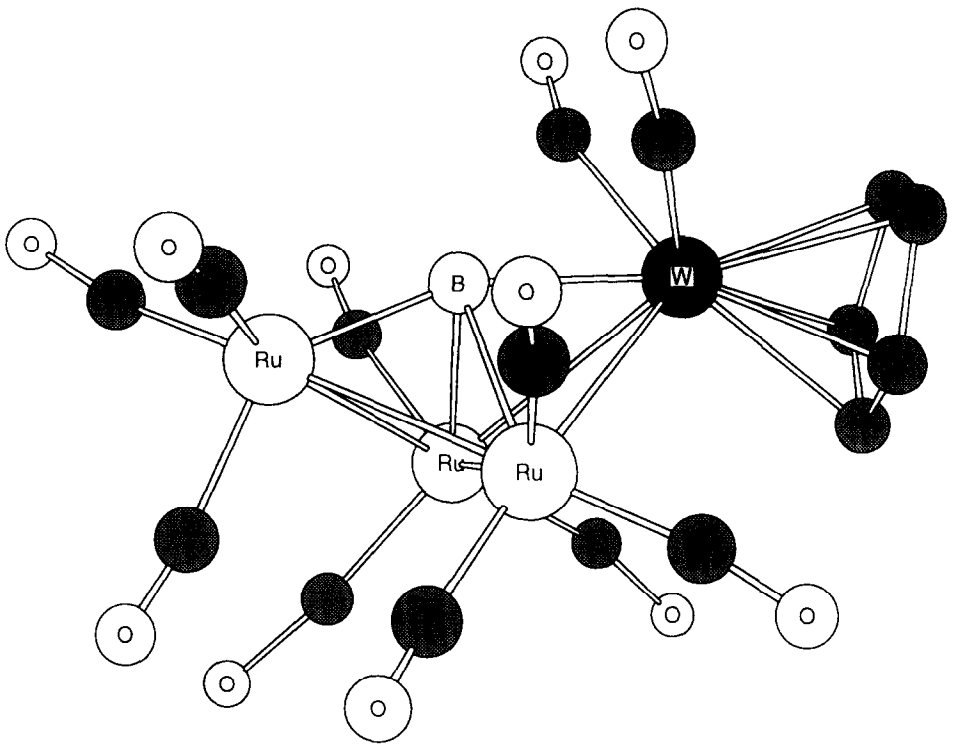

Fig. 8. The structure of $[H\{CpW(CO)_2\}Ru_3(CO)_9BH]$; the two cluster H atoms were not located but spectroscopic data and consideration of the carbonyl ligand orientations support their placements along the $Ru_{hinge}-Ru_{hinge}$ and $Ru_{wingtip}-B$ edges.

a 14 electron fragment for a 15 electron fragment. This is observed in $[H\{CpMo(CO)_2\}Ru_3(CO)_9BH]$ and $[H\{CpW(CO)_2\}Ru_3(CO)_9BH]$. Alternatively, taking $[H\{Cp^*Rh\}Ru_3(CO)_9BH_2]$ and substituting a PPh_3 ligand for CO ligand on one ruthenium atom alters the electron distribution in the cluster and causes the migration of a hydrogen atom away from the boron atom. Again this has the effect of making the boron centre more "boridic" in nature. A word of caution should be given, however: in phosphine substitution reactions in $[HFe_4(CO)_{12}BH]^-$, the reverse is true and a hydrogen atom from an Fe—H—Fe site migrates to a Fe—H—B site. The crucial point is that, again, this represents a movement towards the location of the phosphine ligand (see Section 3.3) [51,64].

3.3. Reactivity

3.3.1. Deprotonation

One way of denuding the boron atom of its hydrogen atoms thereby rendering it more boridic is, obviously, deprotonation, and a comparison of the sequences of deprotonation for the related clusters $[HFe_4(CO)_{12}BH_2]$, $[HFe_4Ru_3CO)_{12}BH_2]$,

$[HRu_4(CO)_{12}BH_2]$ and $[HOs_4(CO)_{12}BH_2]$ is of interest. The cluster core begins in each case with the hydrogen atom arrangement shown in Fig. 7. Fehlner and co-workers have shown that $[HFe_4(CO)_{12}BH_2]$ loses protons according to the sequence given in Eq. 2 [51,53,64,65]; the placement of the H atoms in the formulae indicates whether or not there is a B—H interaction. The success (or failure) of a particular deprotonation step depends not only on the base used but also on the cation [65].

$$[HFe_4(CO)_{12}BH_2] \rightarrow [HFe_4(CO)_{12}BH]^- \rightarrow [Fe_4(CO)_{12}BH]^{2-} \rightarrow [Fe_4(CO)_{12}B]^{3-} \quad (2)$$

In contrast, Shore and co-workers report [31] that $[HRu_4(CO)_{12}BH_2]$ undergoes loss of two protons in the sequence given in Eq. (3); the formation of the monoanion $[HRu_4(CO)_{12}BH]^-$ has been studied independently [32]. The osmium system behaves similarly to its ruthenium counterpart and $[HOs_4(CO)_{12}BH_2]$ loses H^+ according to Eq. (4) [46]. The change in behaviour of these systems on descending the group 8 triad is in accord with predictions made by Fehlner [66,67].

$$[HRu_4(CO)_{12}BH_2] \rightarrow [HRu_4(CO)_{12}BH]^- \rightarrow [HRu_4(CO)_{12}B]^{2-} \quad (3)$$

$$[HOs_4(CO)_{12}BH_2] \rightarrow [HOs_4(CO)_{12}BH]^- \rightarrow [HOs_4(CO)_{12}B]^{2-} \quad (4)$$

The introduction of a heteroatom into the wingtip site of the butterfly array removes the symmetry of the two wingtip sites. This is nicely demonstrated in the deprotonation of $[HFeRu_3(CO)_{12}BH_2]$. The choice for H^+ removal is between an Fe—H—B and Ru—H—B site and, as would be expected on bond enthalpy grounds, it is the iron-associated proton that is removed first [45].

While relatively straightforward, these deprotonations are important steps in activating the semi-interstitial boron atom towards further reaction (see Sections 3.3.4 and 5.1).

3.3.2. Phosphine substitution reactions

We have already noted that the substitution of a PPh_3 for CO ligand in $[H\{Cp^*Rh\}Ru_3(CO)_9BH_2]$ produces $[H_2\{Cp^*Rh\}Ru_3(CO)_8(PPh_3)BH]$ with concomitant migration of one Ru—H—B bridging hydrogen atom to an Ru—H—Ru site [56]. The substitution reaction is facile, occurring almost quantitatively in CH_2Cl_2 solution at room temperature within 1 h. Substitution occurs exclusively at a wingtip ruthenium atom and in an equatorial site.

A range of tertiary phosphine ligands will substitute for CO in $[HRu_4(CO)_{12}BH_2]$, the first site being a wingtip equatorial site and the second site being the other wingtip ruthenium atom, also equatorially centred [68,69]. This same pattern is also observed in the reaction of $[HFe_4(CO)_{12}BH]^-$ with PMe_2Ph, although, as was stated earlier, here the introduction of the second phosphine ligand is accompanied by a rearrangement of the cluster-bound hydrogen atoms [51,64]. The pathway of this reaction has been investigated and an associative process in each substitution step is proposed. Growth and decay of intermediates can be observed by monitoring the reactions with ^{11}B NMR spectroscopy [64].

Interestingly phosphine substitution in $[H_2Ru_5(CO)_{13}Cp^*BH_2]$ (Fig. 6) has the effect of replacing the metal spike and forming $[HRu_4(CO)_{11}(PPh_3)BH_2]$ [57], i.e. the same product that is obtained when $[HRu_4(CO)_{12}BH_2]$ reacts with PPh_3.

3.3.3. Reactions with small unsaturated molecules

The reactions of the carbido and nitrido clusters $[HRu_4(CO)_{12}CH]$ and $[Ru_4(CO)_{12}N]^-$ with alkynes have been documented and exhibit two very different sequences of events. For the semi-interstitial carbide, C—C coupling occurs as $[HRu_4(CO)_{12}CH]$ reacts with PhC≡CPh but the geometry of the Ru_4C framework remains virtually unchanged [30]. On the contrary, when $[Ru_4(CO)_{12}N]^-$ reacts with PhCCPh in the presence of H^+, the alkyne inserts into the hinge bond of the metal skeleton; the nitrogen atom is protonated and is pulled out from its semi-interstitial position [29]. These differing routes find yet another path with which to be contrasted in the reaction of $[HRu_4(CO)_{12}BH_2]$ with PhC≡CPh.

The compound $[HRu_4(CO)_{12}BH_2]$ reacts with PhC≡CPh when photolysed in CH_2Cl_2 solution (16 h) to yield $[HRu_4(CO)_{12}B(H)C(Ph)CHPh]$ (Fig. 9), the structure of which has been confirmed by X-ray crystallography. Three features are of interest: (i) transfer of a cluster H atom to the alkyne occurs, (ii) B—C bond

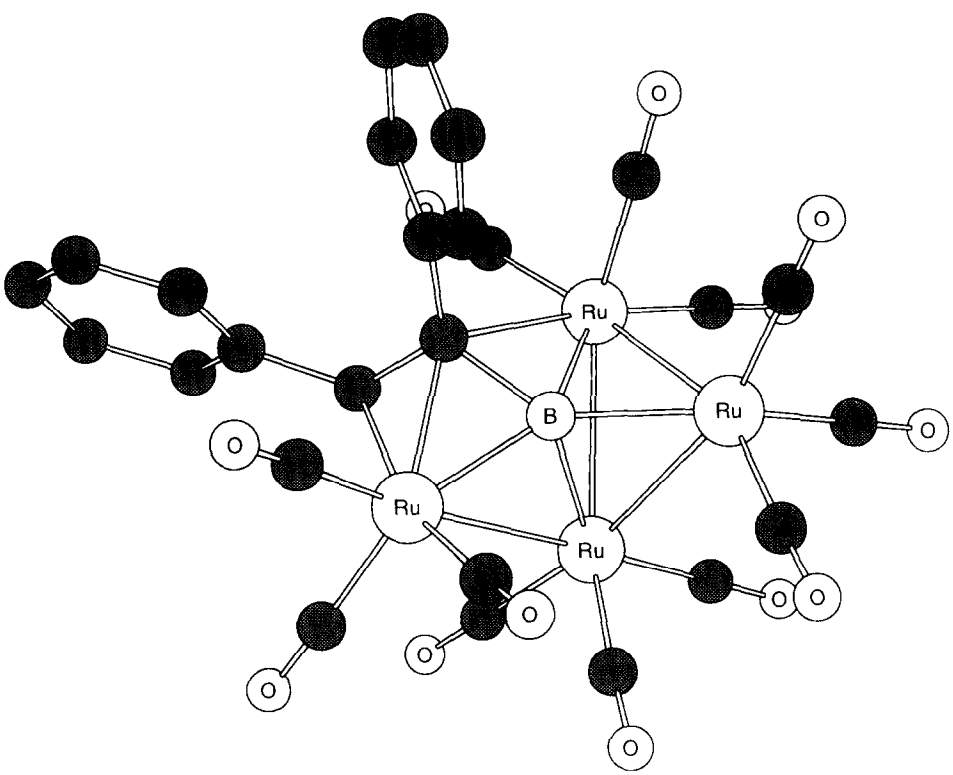

Fig. 9. The structure of $[HRu_4(CO)_{12}B(H)C(Ph)CHPh]$; H atoms are omitted.

formation occurs, and (iii) the Ru_4 butterfly skeleton (usually found to be very robust) is opened along one edge as the alkyne inserts into it [70,71]. A similar reaction occurs when $[HRu_4(CO)_{12}BH_2]$ is photolysed with PhC≡CMe [72].

In marked contrast, the heterometallic boride cluster $[H\{CpW(CO)_2\}Ru_3(CO)_9BH]$ reacts with PhC≡CPh under similar conditions to those just described to yield $[H\{CpW(CO)_2\}Ru_3(CO)_9BC(Ph)CHPh]$ (Fig. 10) in which the Ru_3W skeleton retains its butterfly geometry. Once again, however, transfer of a cluster hydrogen atom to the alkyne and B—C bond formation do occur [71]. These differences have not been fully rationalized.

A novel pathway which competes with the alkyne insertion into the cluster has been observed during the reaction of $[HRu_4(CO)_{12}BH_2]$ with PhC≡CMe: the cyclodimerization of the alkyne to give 1-phenyl-2,3-dimethylazulene (Fig. 11). The nature of this bright blue product has been confirmed by the results of an X-ray diffraction study [72].

Work in our own group has been extended from the alkynes to a range of other unsaturated molecules but without particular success. However, one result, pertinent to this section, was achieved serendipitously. In attempts to synthesize Ru_3MB

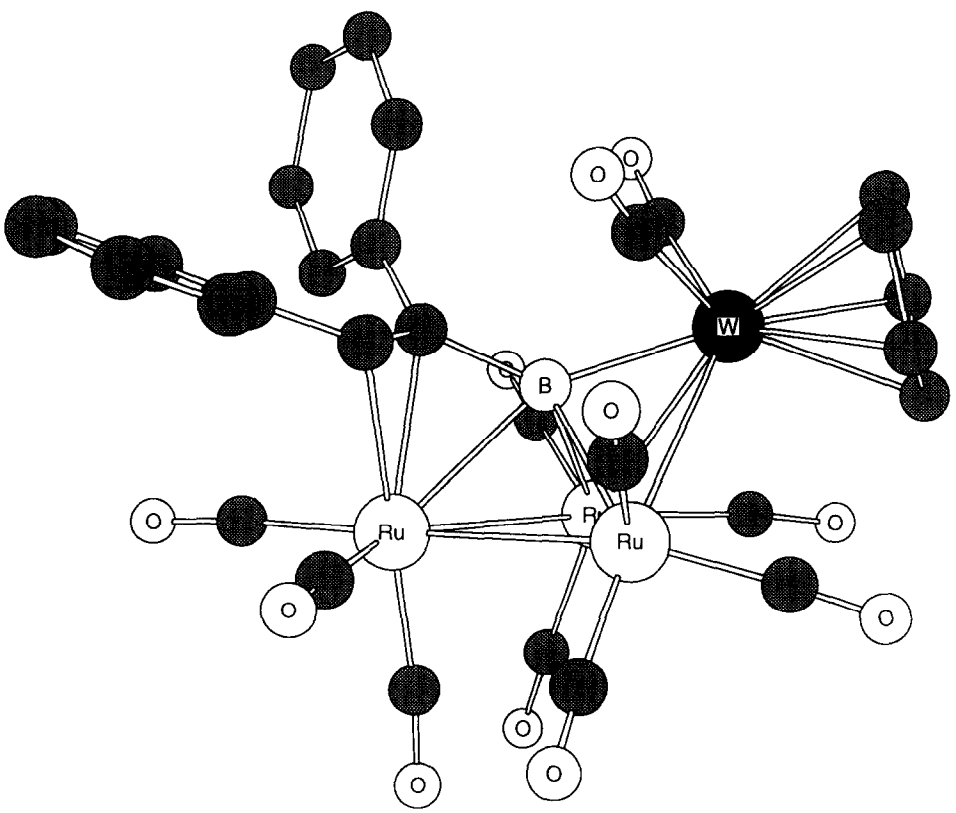

Fig. 10. The structure of $[H\{CpW(CO)_2\}Ru_3(CO)_9BC(Ph)CHPh]$; H atoms are omitted.

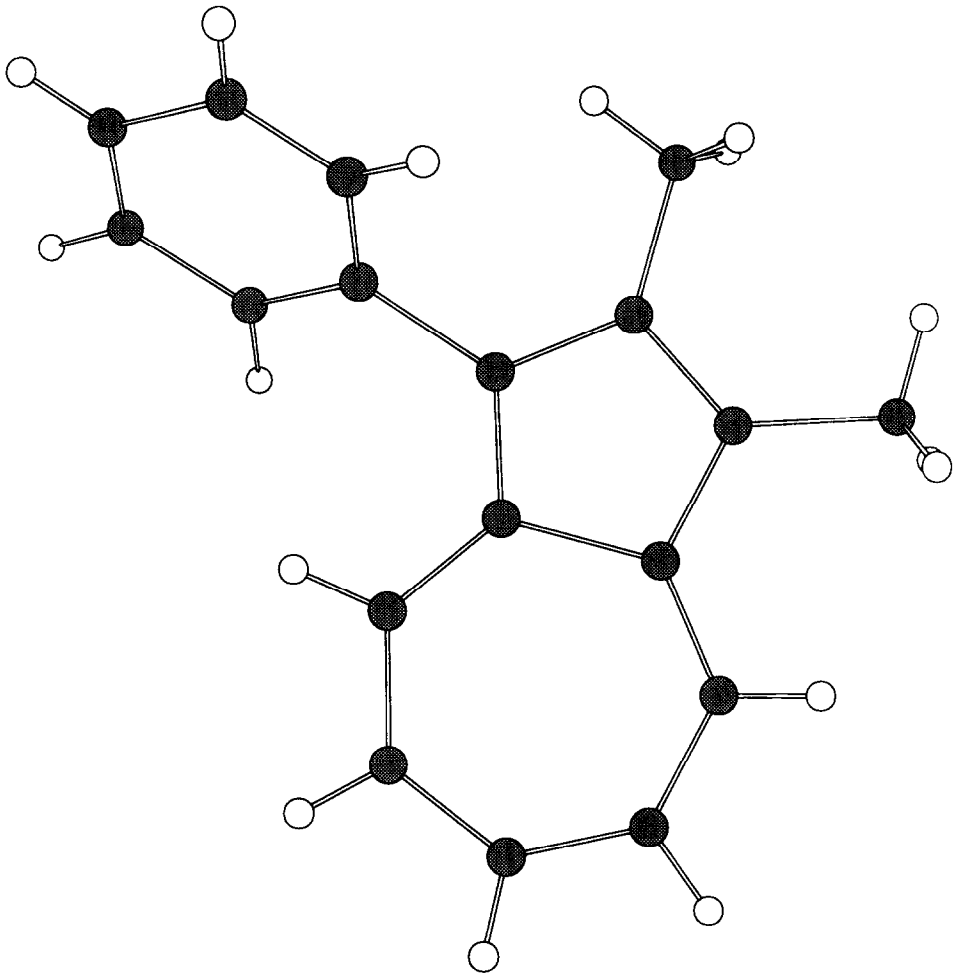

Fig. 11. The structure of 1-phenyl-2,3-dimethylazulene.

butterfly clusters where M is a group 6 metal, the use of $[M(CO)_{6-x}(NCMe)_x]$ (M = Cr, Mo or W) in reactions with $[Ru_3(CO)_9BH_5]$ led to the formation of $[HRu_4(CO)_{12}BH(NCMeH)]$ (Fig. 12). We have shown that this product is not obtained when $[HRu_4(CO)_{12}BH_2]$ is photolysed with MeC≡N. We have proposed that a likely mechanism is via an $\{Ru_3(CO)_9BH_3(NCMe)\}$ intermediate [73], with this species being related to the series of compounds of the type $[H_3Os_3(CO)_9BL]$ (L = two electron donor) isolated by Shore's group [59] and $[HFe_3(CO)_9B(CO)]^{2-}$ reported recently by Fehlner and co-workers [74].

3.3.4. Gold(I) phosphine derivatives

The use of group 11 fragments as cluster building blocks is well established [75]. In isolobal terms, an $\{MPR_3^+\}$ (M = group 11 metal, R = alkyl or aryl) unit is

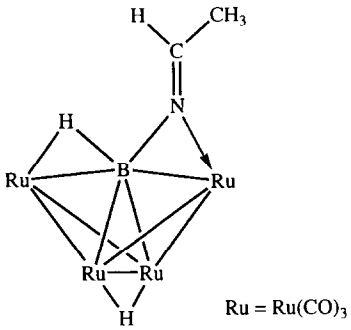

Fig. 12. The structure of $[HRu_4(CO)_{12}BH(NCMeH)]$; a second isomer with the other possible orientation of the N=CMeH group has also been isolated.

considered to replace a proton on a cluster surface. Of course, there are differences, notably the propensity of the gold atoms to aggregate. Group 11 metal units are not representative of the majority of metal fragments. In bonding to a cluster, they tend to mimic hydrogen atoms rather than becoming an integral part of a recognizable polyhedral cluster cage. For this reason, reactions involving the addition of $\{AuPR_3^+\}$ units are discussed here in a single section.

The general reaction given in Eq. (5) can be applied to many cluster anions, not least the butterfly clusters with semi-interstitial boron atoms. These systems have proved to be of significant interest in that Au—B bonds are usually formed in preference to the {AuL} units associating only with the transition metal skeleton.

$$[M_x(CO)_y]^- + [R_3PAuCl] \rightarrow [M_x(CO)_yAuPR_3] + Cl^- \quad (5)$$

Initial reactions in this area centred on the $[HFe_4(CO)_{12}BH]^-$ anion. This reacts smoothly with an excess of $[Ph_3PAuCl]$ to give the digold(I) derivative $[Fe_4(CO)_{12}BH\{AuPPh_3\}_2]$ [76]. The arsine derivative $[Fe_4(CO)_{12}BH\{AuAsPh_3\}_2]$ (Fig. 13) can be prepared similarly [77]. In each derivative, the Fe_4B core is retained, as is one Fe—H—B bridging interaction. One gold(I) unit bridges an $Fe_{wingtip}$—B edge and one interacts with an Fe_{hinge}—B edge. The two gold atoms are within bonding contact of one another: 2.943(1) Å in $[Fe_4(CO)_{12}BH\{AuPPh_3\}_2]$ and 2.931(1) Å in $[Fe_4(CO)_{12}BH\{AuAsPh_3\}_2]$. Electrochemical properties of both of these clusters have been explored. Each undergoes a one-electron reduction and a one-electron oxidation; $[Fe_4(CO)_{12}BH\{AuPPh_3\}_2]$ can be oxidized to the dication [77].

The monogold derivative $[HFe_4(CO)_{12}BH\{AuPPh_3\}]$ has also been prepared but not structurally characterized [78]. Only when we move to a phosphine with a much larger cone angle (i.e. P(*o*-tolyl)$_3$) have we been able to isolate and characterize structurally a monogold compound; in $[HFe_4(CO)_{12}BH\{AuP(o\text{-tolyl})_3\}]$, the gold(I) unit bridges an Fe—H—B edge and Fig. 14 indicates the manner in which the bulk of the P(*o*-tolyl)$_3$ ligand protects the topside of the cluster [79].

While a very sterically demanding phosphine stabilizes a monogold derivative, smaller phosphines have the effect of allowing the digold system to

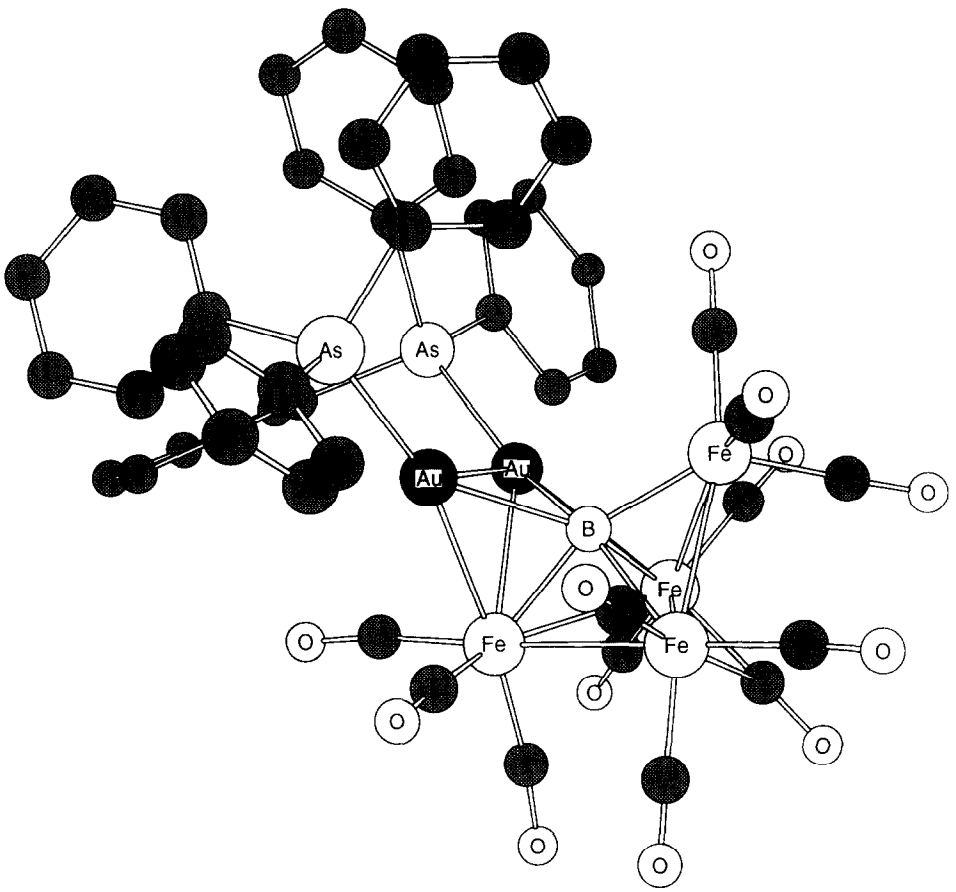

Fig. 13. The structure of $[Fe_4(CO)_{12}BH\{AuAsPh_3\}_2]$; H atoms are omitted.

adopt a new isomeric structure. This was first noted in the formation of $[Fe_4(CO)_{12}BH\{AuPEt_3\}_2]$. The spectroscopic signature (^1H and ^{11}B NMR spectra) of this compound suggests a structure in accordance with that shown in Fig. 13 for $[Fe_4(CO)_{12}BH\{AuAsPh_3\}_2]$. The most characteristic feature is in the ^1H NMR spectrum: a broad signal (a collapsed 1:1:1:1 quartet) at $\delta = -10.4$ indicating the presence of an Fe—H—B interaction. However, the solid state structure tells a different story (Fig. 15); both gold(I) units bridge $Fe_{wingtip}$—B edges and the cluster-bound hydrogen atom now bridges the hinge edge of the butterfly skeleton. Low temperature NMR spectroscopic results corroborate these data, revealing the presence of two isomers in solution [80,81]. This work has been extended to include a wide range of phosphines and illustrates the effects on the isomer distribution of varying the cone angle of the PR_3 group [81]. The cluster cores of the two isomers are compared in Fig. 16.

Replacing the source of gold(I) by the oxonium salt $[\{Ph_3PAu\}_3O][BF_4]$ permits

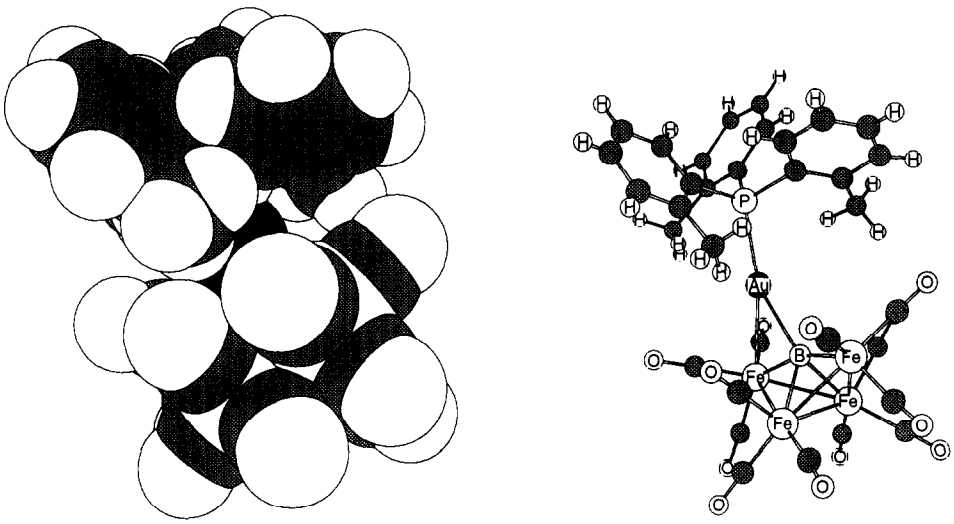

Fig. 14. Two views of the structure of $[HFe_4(CO)_{12}BH\{AuP(o\text{-tolyl})_3\}]$ emphasizing the protective "umbrella" of the bulky phosphine ligand.

high yields of the trigold derivative $[Fe_4(CO)_{12}B\{AuPPh_3\}_3]$ to be obtained (Fig. 17). The results of an X-ray diffraction study confirm that the three gold atoms are adjacent to one another, describing a V-shaped assembly over the top of the boron atom. In this molecule, the boron atom is completely encapsulated and is seven coordinate: a novel observation for an atom with three valence electrons and a testament to the delocalized nature of the bonding in this, and related, clusters. Despite an asymmetrical structure being confirmed in the solid state, the three phosphorus atoms (and by inference the three gold(I) phosphine units) are equivalent in solution on the NMR spectroscopic time scale [82].

Different trends are observed for the tetraruthenium system. The reaction of $[HRu_4(CO)_{12}BH]^-$ with an excess of $[Ph_3PAuCl]$ yields $[HRu_4(CO)_{12}B\{AuPPh_3\}_2]$ but here, unlike the iron analogue, the cluster hydrogen atom is bound to the Ru—Ru hinge edge [32]. The two monodentate phosphine ligands may be replaced by a didentate ligand such as dppf. The {Au—P----P—Au} unit acts like a "basket handle" over the top of the cluster. This is beautifully demonstrated in $[HRu_4(CO)_{12}BAu_2(dppf)]$ (Fig. 18). This compound exhibits interesting solution dynamics involving inversion at the phosphorus atoms and concomitant mutual twisting of the two cyclopentadienyl rings. Movement of the phosphorus atoms causes an associated motion of the two gold atoms from one side of the Ru_4B core to the other. The result is an interconversion of enantiomers [83].

In all the reactions mentioned so far in this section, the Au—P bonds have remained intact. In the interpretation of solution temperature-dependent NMR spectra, it is assumed that Au—P bond cleavage does not occur. While this does indeed seem usually to be the case for these systems, there are two pieces of evidence that urge caution.

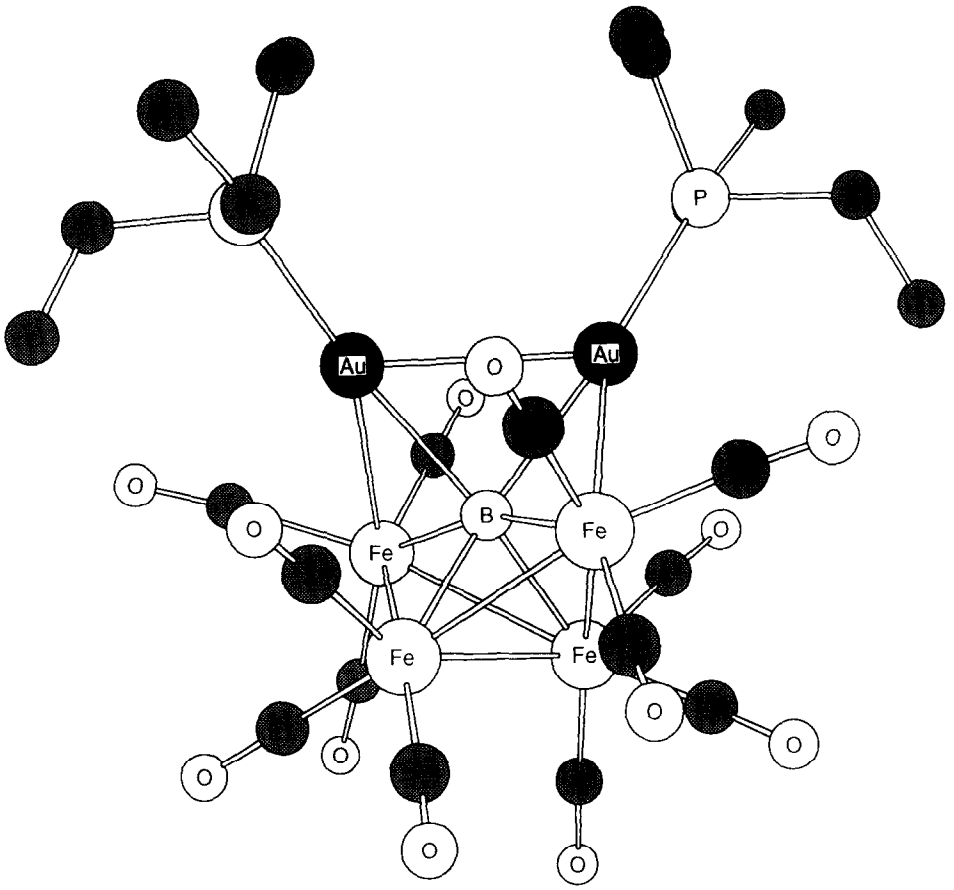

Fig. 15. The structure of the minor isomer of $[HFe_4(CO)_{12}B\{AuPEt_3\}_2]$; H atoms are omitted.

The first is in the preparation of the bis(triethylphosphine)gold(I) derivative from $[PPN][HFe_4(CO)_{12}BH]$ and $[Et_3PAuCl]$. The results of this experiment showed not only that $[Fe_4(CO)_{12}BH\{AuPEt_3\}_2]$ is synthesized as planned, but that mixtures of $[Fe_4(CO)_{12}BH\{AuPPh_3\}_2]$ and $[Fe_4(CO)_{12}BH\{AuPEt_3\}\{AuPPh_3\}]$ are also present. The only source of PPh_3 is the PPN^+ cation [78].

The second point is the observation that, in some reactions of $[HFe_4(CO)_{12}BH]^-$ or $[HRu_4(CO)_{12}BH]^-$ with $[R_3PAuCl]$ (R = various), a competitive pathway exists which produces $[\{HFe_4(CO)_{12}BH\}_2Au]^-$ or $[\{HRu_4(CO)_{12}BH\}_2Au]^-$ respectively (see Section 6).

3.3.5. Other metal fragment additions

Since the additions of metal fragments other than gold(I) to the M_4B core represent synthetic routes to boride clusters with higher nuclearity frameworks, they are dealt with in the appropriate sections below.

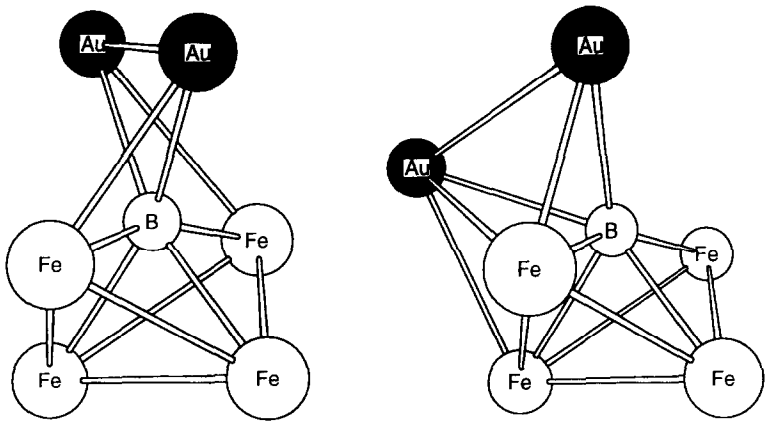

Fig. 16. Comparison of the $\{Fe_4Au_2B\}$ cores of the two isomers of $[HFe_4(CO)_{12}B\{AuPR_3\}_2]$ (see text for R).

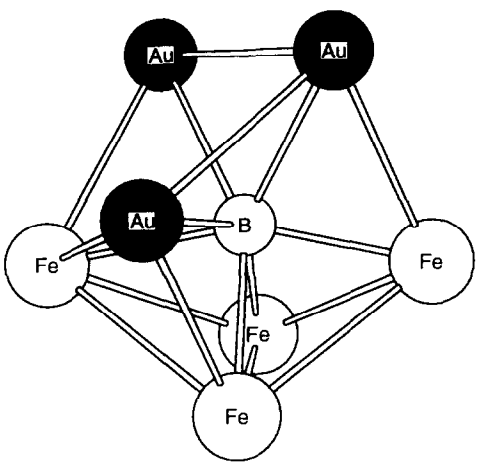

Fig. 17. The structure of the $\{Fe_4Au_3B\}$ core of $[Fe_4(CO)_{12}B\{AuPPh_3\}_3]$.

4. Clusters with five metal atoms

In this section three very different pentametal boride clusters are described. The first is a gold(I) derivative of $[Ru_5(CO)_{15}B]^-$ and as such should really be regarded as a hexametal cage. Attempts to synthesize $[Ru_5(CO)_{15}B]^-$ in a systematic "building-up" process from lower nuclearity ruthenaboranes proved not to be successful [84] but use of a "decapping" technique starting from $[Ru_6(CO)_{17}B\{AuPPh_3\}]$ (see Section 5.2) is an effective way of generating the pentaruthenium boride $[Ru_5(CO)_{15}B\{AuPPh_3\}]$. The conditions of vertex removal are 55 atm CO, overnight in an autoclave. The single-crystal structure of $[Ru_5(CO)_{15}B\{AuPPh_3\}]$ (Fig. 19) confirms a square-based pyramidal array of group 8 metal atoms with the boron

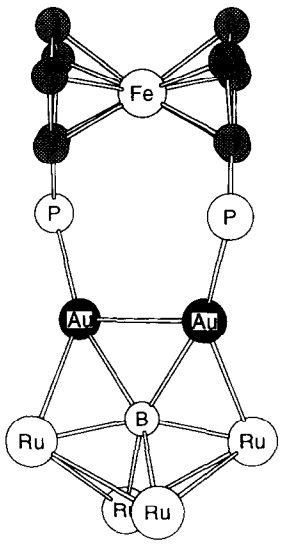

Fig. 18. The core structure $[HRu_4(CO)_{12}BAu_2(dppf)]$; H atoms, carbonyl ligands and the phenyl groups are omitted.

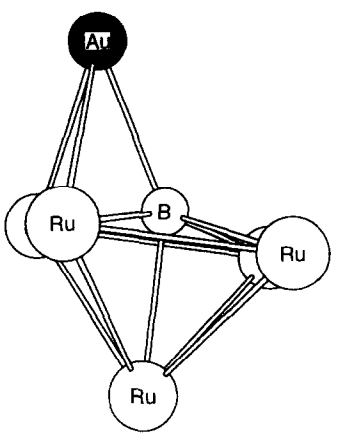

Fig. 19. The $\{Ru_5BAu\}$ core of $[Ru_5(CO)_{15}B\{AuPPh_3\}]$.

atom lying 0.375 Å below the square face; it is within bonding contact of all five ruthenium atoms. The gold(I) fragment is in an unusual position, bridging one basal Ru—Ru edge but pulled inwards by a bonding interaction with the boron atom (Au—B distance, 2.26(5) Å) [85].

The pentaosmium cluster $[HOs_5(CO)_{16}B]$ is prepared in low yield together with $[HOs_4(CO)_{12}BH_2]$ by the thermolysis of $[H_3Os_3(CO)_9B(CO)]$. The bridged-butterfly $\{Os_5B\}$ skeleton (Fig. 20) is unique among boride chemistry reported to date, but has precedent in the carbide species $[Os_5(CO)_{16}C]$ [86] and

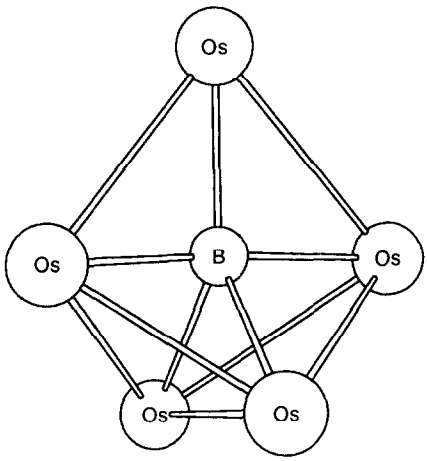

Fig. 20. The $\{Os_5B\}$ core of $[HOs_5(CO)_{16}B]$.

$[Ru_5(CO)_{15}(NCMe)C]$ [87]. The deshielded nature of the boron nucleus is evident from the ^{11}B NMR spectral shift of +184.4. Attempts to deprotonate $[HOs_5(CO)_{16}B]$ have led only to cluster decomposition [46].

Fehlner and co-workers have produced the novel molecular boride $[Co_5(CO)_{14}B(BH)]$ (less than 1% yield) in the reaction of dicobalt octacarbonyl with $BH_3{\cdot}SMe_2$ in toluene (75 °C, 15 min). The major product is $[Co_4(CO)_{12}]$. Two very different boron environments are evident from the ^{11}B NMR spectrum of $[Co_5(CO)_{14}B(BH)]$ and a crystal structure determination reveals the core structure shown in Fig. 21. This is best described as a cobalt-capped Co_4B_2 octahedron with a trans arrangement of boron atoms. The latter, however, are only 1.85(4) Å apart, a distance that is consistent with a B—B bonding interaction. One boron atom possesses a terminal hydrogen atom while the other is in contact with five cobalt

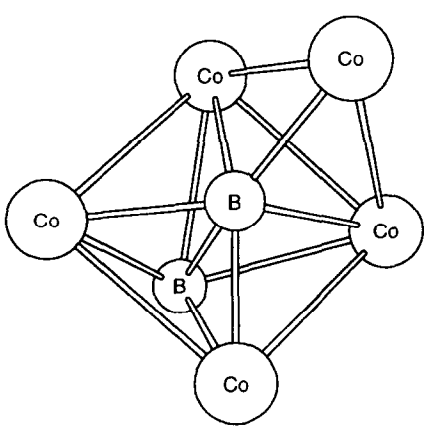

Fig. 21. The $\{Co_5B_2\}$ core of $[Co_5(CO)_{14}B(BH)]$.

atoms and is boridic in nature. The structural preference is strange indeed and has been discussed in terms of the geometric restrictions of cobalt vs. boron [88].

The reaction chemistry of these pentametal systems has yet to be developed.

5. Clusters containing fully interstitial boron atoms

5.1. Synthesis and structure

The fully interstitial borides are found within octahedral and trigonal prismatic interstices as shown in Fig. 1, although the irregular $\{Fe_4Au_3\}$ cage present in $[Fe_4(CO)_{12}B\{AuPPh_3\}_3]$ does completely encapsulate a boron atom [82].

Methods of synthesis are varied but most involve the "building-block" approach starting with an $\{M_3B\}$, $\{M_3B_2\}$ or $\{M_4B\}$ core. We deal first with the homometallic clusters, although historically the heterometallic anion $[Fe_4Rh_2(CO)_{16}B]^-$ was the first true closed polyhedral boride to be fully characterized (see below).

In 1975, Schmid *et al.* reported the formation of a species proposed to be $[Co_6(CO)_{18}B]$ from the reactions of either $Co_2(CO)_8$ and BBr_3 (60 °C) or $Co_2(CO)_8$ with B_2H_6 under pressure [89]. It is noticeable that this formulation gives an electron count of 93; it therefore not only is an odd electron species, but fits the electron counts of neither the trigonal prism (90 electrons) nor the octahedron (86 electrons).

The first report of an octahedral hexaruthenium boride cluster came from Shore and co-workers [47]; $[HRu_6(CO)_{17}B]$ was prepared by treating triruthenium dodecacarbonyl with BH_3·thf in toluene (75 °C). The reaction of $[Ru_3(CO)_{12-x}(NCMe)_x]$ ($x=1$ or 2) with BH_3·thf in the presence of NMe_3 provides one route to the anion $[Ru_6(CO)_{17}B]^-$ (about 10% yield); the second product in this synthesis is the unusual donor–acceptor complex $[HRu_3(CO)_{10}(\mu\text{-}COBH_2NMe_3)]$ [48]. The formulation of $[Ru_6(CO)_{17}B]^-$ is consistent with an 86 electron octahedron, but structural confirmation of the octahedral cage was provided by the Shore group for the conjugate acid [47]. In the solid state, a second isomer of $[HRu_6(CO)_{17}B]$ has been elucidated (Fig. 22) [45] which differs from the first principally in the arrangement of the carbonyl ligands. The differences in structure are too great for the two species to be simply regarded as polymorphs. In solution, the IR spectra of the two isomers are different. The boron atom in $[HRu_6(CO)_{17}B]$ resides at the very heart of the octahedral cavity and interacts equally with all six metal atoms. The second isomer of $[HRu_6(CO)_{17}B]$ is a result of the cluster assembly described earlier in Section 3.1 and Fig. 4. In addition to envelopes assigned to the hexametal boride, a high mass envelope was observed at $m/z=1575$ in the mass spectrum of $[HRu_6(CO)_{17}B]$. The formation of $[Ru_9(CO)_{23}B_2]$ has been proposed; this formulation is consistent with a cluster that possesses a 124 valence electron face-sharing bioctahedral structure [45].

A systematic approach to the formation of $[HRu_6(CO)_{17}B]$ or to its conjugate base is to "sandwich" together $\{Ru_3\}$ and $\{Ru_3B\}$ units. This paper exercise is brought to life most effectively, not with $[Ru_3(CO)_9BH_4]^-$ (possessing a tetrahedral Ru_3B core) as a precursor, but with $[Ru_3(CO)_9B_2H_5]^-$ (possessing a square-based

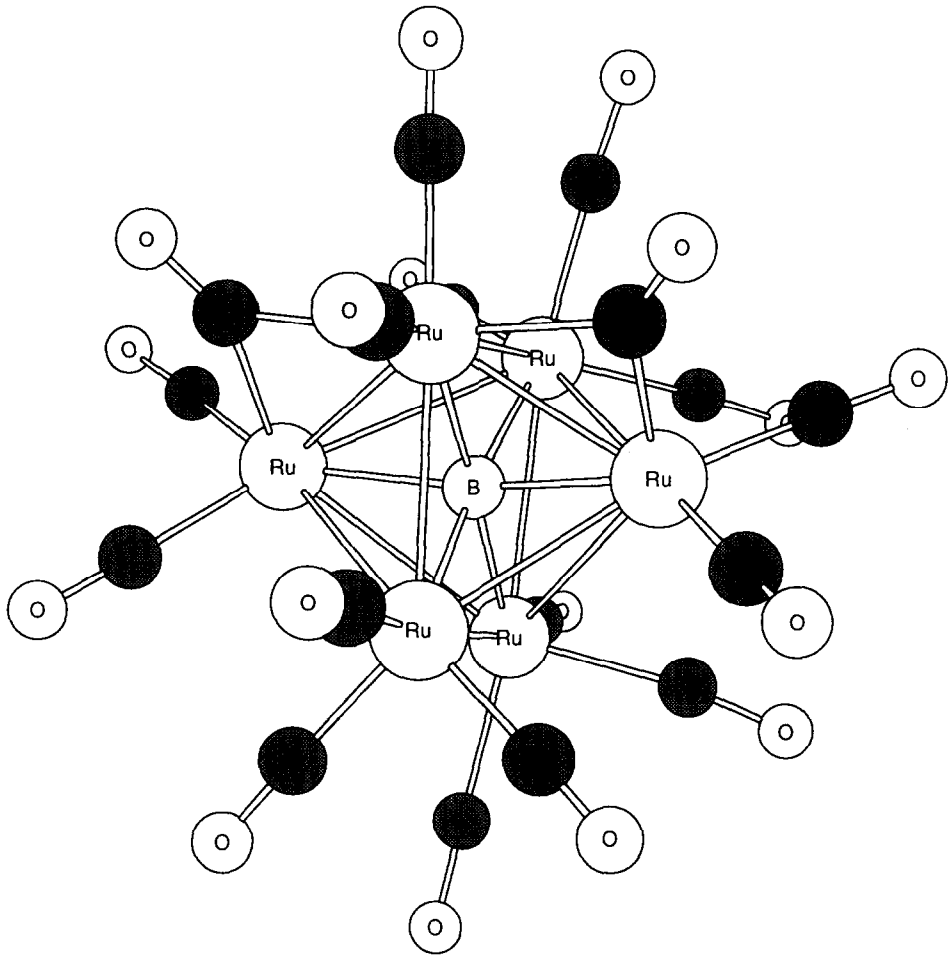

Fig. 22. The structure of one isomer of $[HRu_6(CO)_{17}B]$ [45]; the second isomer [47] differs principally in the CO ligand arrangement.

pyramidal Ru_3B_2 core with the three ruthenium atoms defining a triangular face). The reaction of $[Ru_3(CO)_9B_2H_5]^-$ with $[Ru_3(CO)_{10}(NCMe)_2]$ leads to the formation of $[Ru_6(CO)_{17}B]^-$ (about 10% yield) and, in addition, to the trigonal prismatic boride anion $[H_2Ru_6(CO)_{18}B]^-$ (Fig. 23) (about 20% yield) [34,35]. The observation that these two cluster geometries (Fig. 24) can be formed in the same reaction pot is interesting and begs the question of possible mechanism. The octahedral cluster is characterized by having 86 electrons while the trigonal prismatic boride requires 90 valence electrons. Some evidence of trigonal prism→octahedron cage conversion is apparent in the reaction chemistry of $[H_2Ru_6(CO)_{18}B]^-$ (see Section 5.2).

Recently, Fehlner and co-workers [90] have prepared and structurally

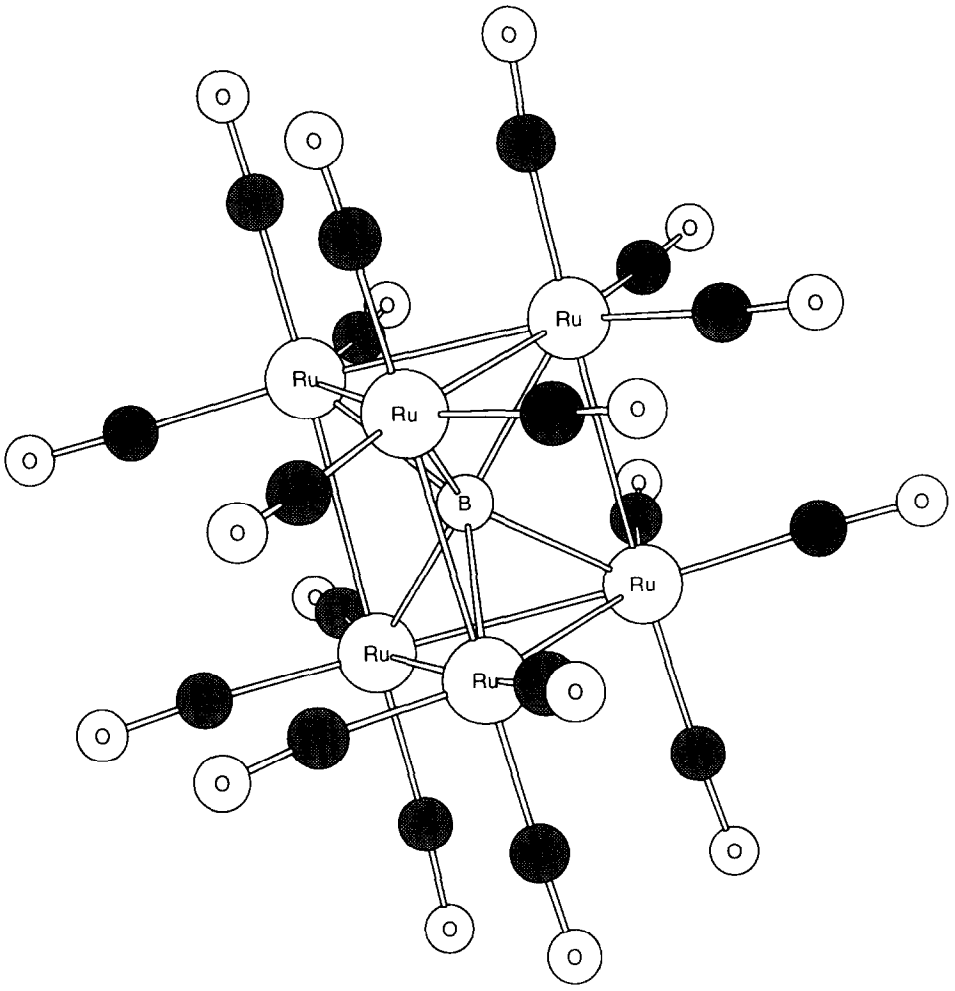

Fig. 23. The structure of $[H_2Ru_6(CO)_{18}B]^-$; hydrogen atoms are omitted.

characterized $[Ph_4As]_2[HFe_7(CO)_{20}B]$. The dianionic cluster has a capped trigonal prismatic structure, with the boron atom residing within the prismatic cavity. The synthetic route to $[HFe_7(CO)_{20}B]^{2-}$ involves the reaction of $[Fe_4(CO)_{12}BH]^{2-}$ with $Fe_2(CO)_9$ or $Fe(CO)_3L$ (L = *cis*-cyclooctene). Two further products in the reaction are the dianions $[Fe_5(CO)_{15}B]^{2-}$ (related to $[Os_5(CO)_{16}B]$; see Section 4) and $[HFe_6(CO)_{17}B]^{2-}$, for which a *nido* geometry has been proposed.

Since, as Fig. 2 showed, the M_4 butterfly framework is a fragment of the octahedron, the addition of two metal atoms to the former should, in principle, close the cage up and generate the latter. This has been neatly demonstrated by the Fehlner group in the reaction of $[HFe_4(CO)_{12}BH]^-$ with $[\{Rh(CO)_2Cl\}_2]$ which yields the *closo* anion $[Fe_4Rh_2(CO)_{16}B]^-$. This reaction has been studied in great detail

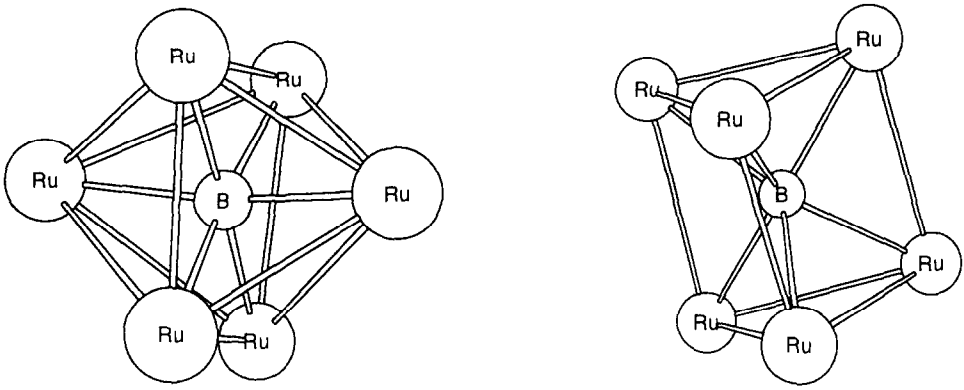

Fig. 24. A comparison of the octahedral and trigonal prismatic $\{Ru_6B\}$ cores from $[HRu_6(CO)_{17}B]$ and $[H_2Ru_6(CO)_{18}B]^-$.

[91–93], particular interest being sparked off by the fact that a cis→trans-Fe_4Rh_2 isomerization occurs during the reaction. The process can be monitored by using ^{11}B NMR spectroscopy where a triplet ($\delta = +205$, $J_{Rh-B} = 23.3$ Hz) assigned to the cis isomer gives way to a second triplet ($\delta = +211$, $J_{Rh-B} = 25.8$ Hz) assigned to the trans species (Fig. 25). There is also spectral evidence for a pentametal species early on in the reaction. The trans arrangement of the rhodium atoms has been confirmed by a single-crystal X-ray diffraction study. The kinetics of the cis→trans isomerization has been investigated, and the data support a mechanism that is promoted by the presence of a Lewis base. Possible skeletal rearrangements have been discussed by Fehlner and co-workers [92,93]. The protonation of $[Fe_4Rh_2(CO)_{16}B]^-$ leads, first, to the conjugate acid and then to the unexpected neutral product, namely $[H_2Fe_3Rh_3(CO)_{15}B]$. Again, this is an 86 electron, octahedral boride cluster but in the solid state, disorder problems are encountered. From the data, however, it is possible to say that a *mer* arrangement of metal atoms is preferred [93].

A reaction which parallels the formation of $[Fe_4Rh_2(CO)_{16}B]^-$ is that of $[HRu_4(CO)_{12}BH]^-$ with $[\{Rh(CO)_2Cl\}_2]$ to yield $[Rh_2Ru_4(CO)_{16}B]^-$ [94,95]. Here, a preference for the trans arrangement of rhodium atoms is again observed. The boride anion *trans*-$[Ir_2Ru_4(CO)_{16}B]^-$ can be formed in a similar process but in this case there is no spectroscopic evidence for a cis intermediate [95].

The $[Rh_2Ru_4(CO)_{16}B]^-$ anion is also produced (about 15% yield) when $[Ru_3(CO)_9BH_4]^-$ is treated with $[\{Rh(CO)_2Cl\}_2]$. The crystal structure of the anion (as the PPN^+ salt) has been determined, and a trans arrangement of rhodium atoms has been elucidated. Of interest in this reaction is the formation not only of the anionic cluster but of its conjugate acid, $[HRh_2Ru_4(CO)_{16}B]$ (about 10% yield). Probably the most intriguing compound formed in this reaction, however, is $[Rh_3Ru_6(CO)_{23}B_2]^-$. The metal skeleton is that of a capped double trigonal prism, illustrated (in part) in Fig. 26. As is to be expected, some ambiguity exists in the crystal structure over the Rh and Ru positions but a convincing argument can be made for the capping metal being a rhodium atom, and for the remaining ruthenium

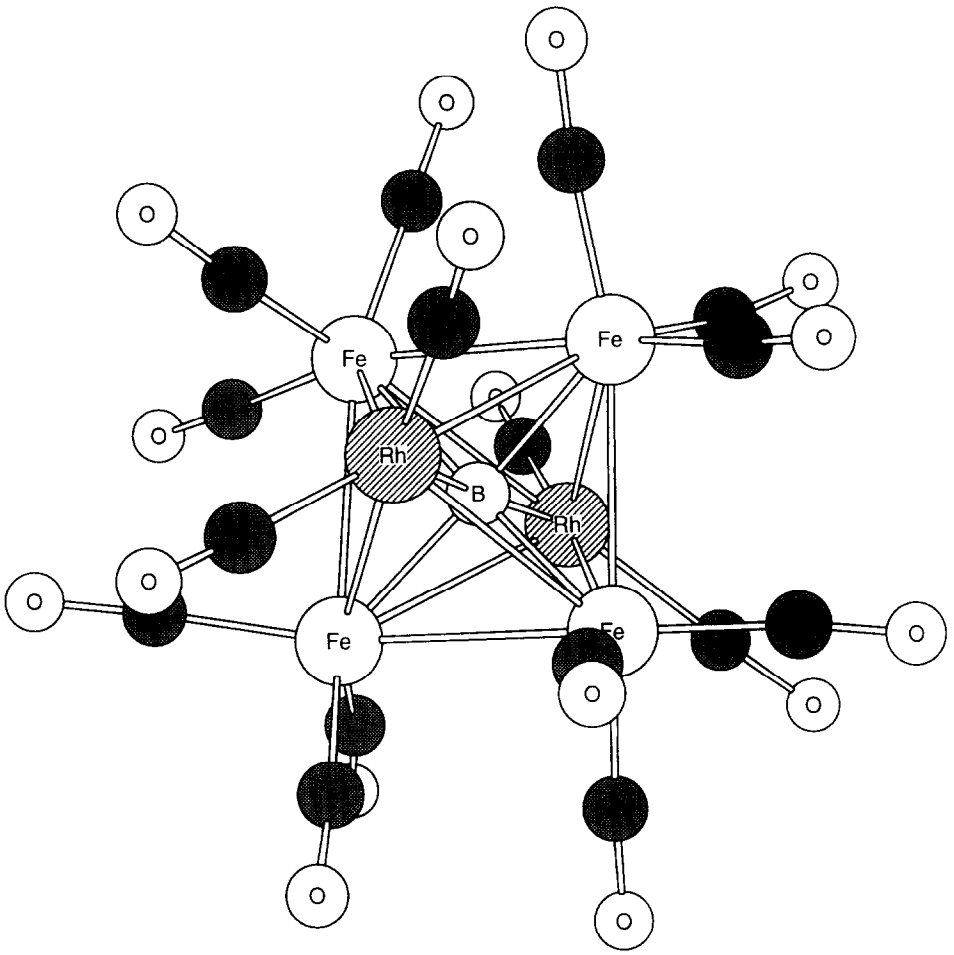

Fig. 25. The structure of the anion *trans*-$[Fe_4Rh_2(CO)_{16}B]^-$.

and rhodium atoms being distributed as shown in Fig. 26. The B—B separation in $[Rh_3Ru_6(CO)_{23}B_2]^-$ is 1.80(2) Å, similar to the distance found in $[Co_5(CO)_{14}B(BH)]$ (see Section 4) and indicative of some B—B bonding interaction (a line joining the B—B atoms in Fig. 26 has been omitted for clarity) [58].

5.2. *Reactivity*

Since the boron atom is buried (and consequently so well protected) within the interstice of an octahedral or trigonal prismatic cage, reactions of the fully interstitial boride clusters tend to centre on the metal carbonyl cage itself. This clearly contrasts with the reactivity patterns of the semi-interstitial clusters described in Section 3.

Deprotonation of $[HRu_6(CO)_{17}B]$ can be readily achieved by treatment using

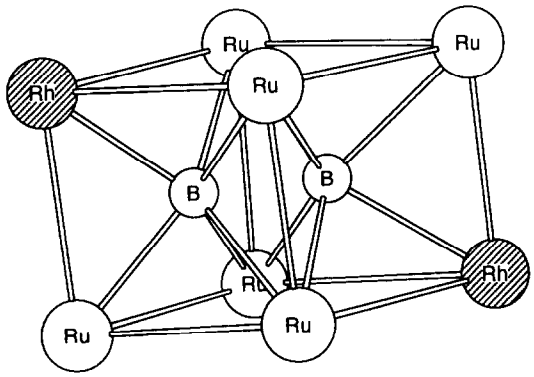

Fig. 26. The $\{Rh_2Ru_6B_2\}$ double prism that constitutes the central core of the $[Rh_3Ru_6(CO)_{23}B_2]^-$ anion.

[PPN]Cl in methanol [47]. The conjugate base [47,48] reacts with $[Ph_3PAuCl]$ or $[(o\text{-tolyl})_3PAuCl]$ to give $[Ru_6(CO)_{17}B\{AuPPh_3\}]$ or $[Ru_6(CO)_{17}B\{AuP(o\text{-tolyl})_3\}]$ respectively [35]. The crystal structure of $[Ru_6(CO)_{17}B\{AuP(o\text{-tolyl})_3\}]$ has been elucidated and the structural results illustrate that the octahedral Ru_6B core is retained during the addition of the gold(I) unit. The latter bridges an Ru—Ru edge of the central octahedral core. When the trigonal prismatic cluster anion $[H_2Ru_6(CO)_{18}B]^-$ is treated with $[Ph_3PAuCl]$, simple addition of one gold unit does not occur. Instead, gold(I) addition is accompanied by loss of hydrogen and carbon monoxide and the products are $[Ru_6(CO)_{17}B\{AuPPh_3\}]$, $[HRu_6(CO)_{16}B\{AuPPh_3\}_2]$ and $[Ru_6(CO)_{16}B\{AuPPh_3\}_3]$. Each cluster has an octahedral core: the loss of ligands is reflected in the change in metal skeleton as the cluster electron count is reduced from 90 to 86. Other reactions in this series have been studied [35], and in no case has it been possible to obtain a derivative which retains the boron-containing trigonal prismatic cage of the precursor $[H_2Ru_6(CO)_{18}B]^-$.

Gold(I) phosphine derivatives of the octahedral clusters $[Rh_2Ru_4(CO)_{16}B]^-$ and $[Ir_2Ru_4(CO)_{16}B]^-$ have been prepared and fully characterized. Crystallographic studies show that, in $[Rh_2Ru_4(CO)_{16}B\{AuP(c\text{-}C_6H_{11})_3\}]$, the rhodium atoms are mutually trans and the gold(I) unit caps one $RhRu_2$ face of the central octahedral boron-containing core. In contrast, in $[Ir_2Ru_4(CO)_{16}B\{AuP(c\text{-}C_6H_{11})_3\}]$, the two iridium atoms adopt a cis arrangement with the gold(I) unit bridging the Ir—Ir edge. There is an interesting contrast between the positions of the group 9 atoms in the cages of $[Rh_2Ru_4(CO)_{16}B]^-$ and $[Ir_2Ru_4(CO)_{16}B]^-$, and their site preferences in the gold(I) phosphine derivatives [95].

Degradation of the octahedral cage in $[Ru_6(CO)_{17}B\{AuPPh_3\}]$ to form $[Ru_5(CO)_{15}B\{AuPPh_3\}]$ was mentioned in Section 4. The reaction is a useful way of accessing the pentaruthenium boride [85].

Other reactions have included boride cluster linkage through the use of difunctional {Au(P---P)Au} units containing didentate phosphine ligands [94].

6. Fusion of boride clusters

The fusion of cluster subunits provides a method of increasing cluster size. Fusion (as opposed to the linkage of boride clusters via, for example, a didentate ligand [68,94]) is taken here to refer to the intimate association of two cluster subunits to generate a new cluster species. If the point of fusion directly involves the boron atom, novel environments are often observed.

The diferraborane $[Fe_2(CO)_6B_2H_6]$ was reported by Fehlner and co-workers some time ago [50,96]. Each of the two boron atoms bears a terminal hydrogen atom. Treatment with *n*-BuLi under controlled reaction conditions results in the formation of $Li_2[Fe_2(CO)_6B_2H_4]$. Further reaction with $Fe(CO)_4Br_2$ leads to the oxidative fusion of two Fe_2B_2 cluster units and the formation of $[\{Fe_2(CO)_6B_2H_4\}_2]$ (Fig. 27):

$$2[Fe_2(CO)_6B_2H_4]^{2-} \xrightarrow{\text{oxidative coupling}} [\{Fe_2(CO)_6B_2H_4\}_2] \quad (6)$$

The fusion process results in the creation of a more boride-like centre in each subcluster in that a terminal hydrogen connection is lost. However, an encapsulated environment is not generated as is evident from the ^{11}B NMR spectral shifts: in $[\{Fe_2(CO)_6B_2H_4\}_2]$, there are two boron environments, characterized by two ^{11}B NMR spectral signals at $\delta = +0.8$ and -2.55 (compare with values listed in Table 1) [97]. In a full report of this study, a distinction is made between kinetically and thermodynamically preferred isomers of $[\{Fe_2(CO)_6B_2H_4\}_2]$ [98]. The reaction of $Li_2[Fe_2(CO)_6B_2H_4]$ with $FeCl_2$ and then $FeCl_3$ leads to the formation of the *B,Fe-conjuncto* cluster (the initially reported isomer). Thermolysis of this isomer allows conversion to the *B,B-conjuncto* system which, in solution, exists as a mixture of three tautomers. The results of single-crystal X-ray diffraction studies of both the *B,Fe* and *B,B* isomers have been described.

Fusion of two cluster subunits, each of which contains a semi-interstitial boron atom, can be achieved using group 11 metal atoms. In Section 3.3.4, the addition of gold(I) phosphine units to anionic boron-containing butterfly clusters was reviewed. In one of these reactions, namely that between $[Ph_2MePAuCl]$

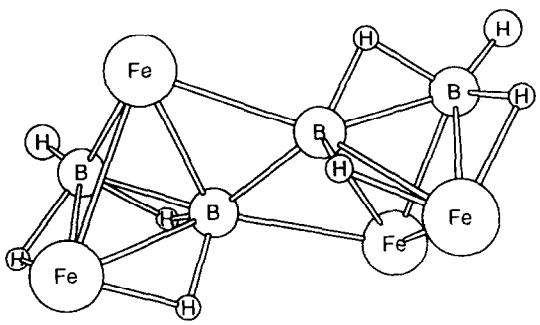

Fig. 27. The coupled cage of one isomer of $[\{Fe_2(CO)_6B_2H_4\}_2]$ (carbonyl ligands omitted) showing fusion utilizing two B—Fe bonds.

and $[HFe_4(CO)_{12}BH]^-$, we observed, not the formation of the expected $[Fe_4(CO)_{12}B\{AuPMePh_2\}_{3-x}H_x]$ ($x=1$–3) type of molecule (see Section 3.3.4), but the production of the ionic compound $[\{HFe_4(CO)_{12}BH\}_2Au][Au(PMePh_2)_2]$. The anion (Fig. 28(a)) exhibits a cis arrangement of cluster subunits although there is a spiro twist at the gold(I) centre. The gold atom may be described as being in a pseudolinear geometry and involved in two three-centre two-electron Fe—Au—B bonding interactions [79,99]. Interestingly, when the structure of the analogous anion $[\{HRu_4(CO)_{12}BH\}_2Au]^-$ was elucidated, it was found to exhibit a trans arrangement of cluster subunits (Fig. 28(b)); $[\{HRu_4(CO)_{12}BH\}_2Au]^-$ may be isolated as the PPN^+ salt from the reactions of $[HRu_4(CO)_{12}BH]^-$ with a range of compounds of the type [ClAu(L—L)AuCl] where L—L is a didentate bis-phosphine ligand [79].

The reaction of $[HRu_4(CO)_{12}BH]^-$ with $[Ag(NCMe)_4][BF_4]$ yields $[\{HRu_4(CO)_{12}BH\}_2Ag]^-$. Like the gold(I) analogue, $[\{HRu_4(CO)_{12}BH\}_2Ag]^-$ possesses a centre of inversion; the cluster subunits are fused in a trans fashion about the silver(I) centre [94]. With $[Cu(NCMe)_4][BF_4]$, $[HRu_4(CO)_{12}BH]^-$ reacts to yield a most novel fused product: $[\{HRu_4(CO)_{12}BH\}_2Cu_4(\mu\text{-Cl})]$ (Fig. 29) [100]. The silver analogue has been observed as a second product in the reaction of $[HRu_4(CO)_{12}BH]^-$ with $[Ag(NCMe)_4][BF_4]$ [94]. In $[\{HRu_4(CO)_{12}BH\}_2Cu_4(\mu\text{-Cl})]$, each boron atom is within bonding contact of seven metal atoms: three copper and four ruthenium centres. The coordination geometry about each boron atom is not unlike that in $[Fe_4(CO)_{12}B\{AuPPh_3\}_3]$ [82] (see Section 3.3.4). Apart from the unexpected nature of this product and the cluster assembly that has occurred

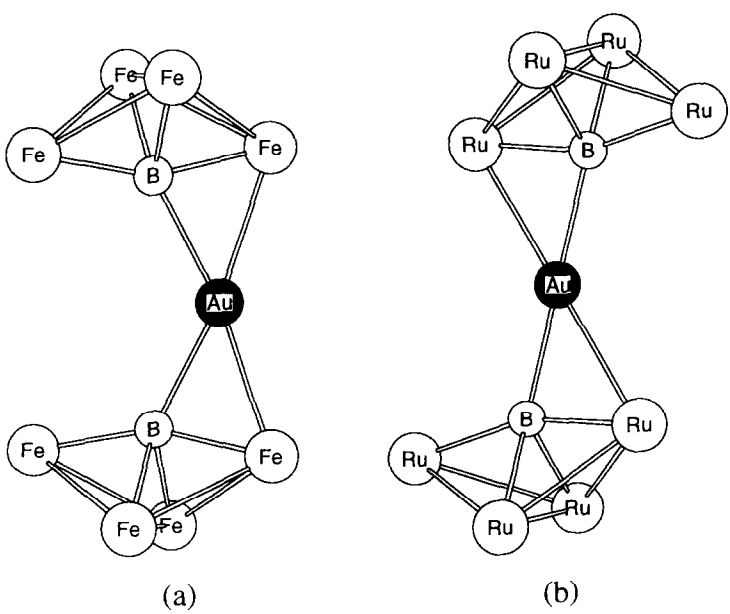

Fig. 28. The $\{(M_4B)_2Au\}$ cluster cores of (a) $[\{HFe_4(CO)_{12}BH\}_2Au]^-$ and (b) $[\{HRu_4(CO)_{12}BH\}_2Au]^-$.

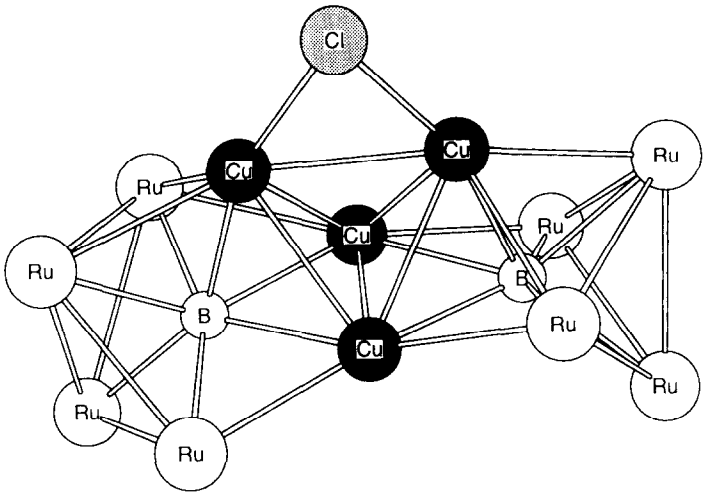

Fig. 29. The $\{(Ru_4B)_2Cu_4(\mu\text{-}Cl)\}$ cluster core of $[\{HRu_4(CO)_{12}B\}_2Cu_4(\mu\text{-}Cl)]$.

during the reaction, an unusual feature of $[\{HRu_4(CO)_{12}BH\}_2Cu_4(\mu\text{-}Cl)]$ is that it exhibits an ambiguity with respect to the oxidation states of the copper centres. Each subcluster formally carries a 2− charge, leaving the central $Cu_4(\mu\text{-}Cl)$ unit to carry a 4+ charge. In addition, this neutral cluster of clusters co-crystallizes with [PPN]Cl (the PPN^+ counterion originates from the cluster starting material).

7. Concluding remarks

Over the past few years, the work of Fehlner and Shore together with our own research efforts have demonstrated a new and intriguing area of transition metal cluster chemistry. To date, the clusters have tended to involve metals from group 8 although Fehlner's work illustrates too that cobalt-containing systems are viable targets. Judging from the wealth of known carbide (and to a lesser extent nitride) cluster species in the literature, the chemistry of the molecular boride cluster should continue to flourish. The reactivity of the semi-interstitial and interstitial boron atom has yet to be developed to its full capacity, and the link to the solid state is of particular interest.

Acknowledgements

The structural pictures for this review have been redrawn, mostly using atomic coordinates taken from the Cambridge Crystallographic Data Base, implemented through the ETH, Zürich [101].

My own contributions to this area of research would not have been possible without the enthusiastic work of my postdoctoral associates, and graduate and

undergraduate project students whose names appear in the references. Also, the geometrical features would not have been confirmed without the collaborative work of Arnie Rheingold (University of Delaware). Financial support has come from the Petroleum Research Fund, administered by the American Chemical Society, and the SERC has provided studentships in Cambridge.

References

[1] C.E. Housecroft, Polyhedron, 6 (1987) 1935.
[2] T.P. Fehlner, New J. Chem., 12 (1988) 307.
[3] T.P. Fehlner, Adv. Inorg. Chem., 35 (1990) 199.
[4] A.A. Aradi and T.P. Fehlner, Adv. Organomet. Chem., 30 (1990) 189.
[5] C.E. Housecroft, Adv. Organomet. Chem., 33 (1991) 1.
[6] C.E. Housecroft, in T.P. Fehlner (ed.) Inorganometallic Chemistry, Modern Inorganic Chemistry Series, Plenum, New York, 1992, Chap. 3, p. 73.
[7] D.P. Workman and S.G. Shore, in G.A. Olah, K. Wade and R.E. Williams (eds.), Electron Deficient Boron and Carbon Clusters, Willey, New York, 1991, Chap. 10, p. 237.
[8] J.D. Kennedy, Prog. Inorg. Chem., 32 (1984) 519; Prog. Inorg. Chem., 34 (1986) 211.
[9] C.E. Housecroft, Boranes and Metallaboranes: Structure, Bonding and Reactivity, Ellis Horwood, Hemel Hempstead, 2nd edn., 1994.
[10] R.N. Grimes (ed.), Metal Interactions with Boron Clusters, Plenum, New York, 1982.
[11] R.P. Ziebarth and J.D. Corbett, J. Am. Chem. Soc., 107 (1985) 4571; 109 (1987) 4844.
[12] M.R. Bond and T. Hughbanks, Inorg. Chem., 31 (1992) 5015.
[13] J.S. Bradley, Adv. Organomet. Chem., 22 (1983) 1.
[14] E.L. Muetterties, Prog. Inorg. Chem., 28 (1981) 203.
[15] M.D. Vargas and J.N. Nicholls, Adv. Inorg. Chem. Radiochem., 30 (1986) 123.
[16] W.L. Gladfelter, Adv. Organomet. Chem., 24 (1985) 41.
[17] V.G. Albano, D. Braga and S. Martinengo, J. Chem. Soc., Dalton Trans., (1986) 981.
[18] B.T. Heaton, L. Strona, S. Martinengo, D. Strumolo, V.G. Albano and D. Braga, J. Chem. Soc., Dalton Trans., (1983) 2175, and references cited therein.
[19] G. Ciani and S. Martinengo, J. Organomet. Chem., 306 (1986) C49.
[20] S. Martinengo, G. Ciani, A. Sironi, B.T. Heaton and J. Mason, J. Am. Chem. Soc., 101 (1979) 7095.
[21] S.B. Colbran, F.J. Lahoz, P.R. Raithby, J. Lewis, B.F.G. Johnson and C.J. Cardin, J. Chem. Soc., Dalton Trans., (1988) 173.
[22] J. Vidal, W.E. Walker, R.L. Pruett and R.C. Schoening, Inorg. Chem., 18 (1979) 129.
[23] J. Vidal, Inorg. Chem., 20 (1981) 243.
[24] J. Vidal and J.M. Troup, J. Organomet. Chem., 213 (1981) 351.
[25] K. Whitmire and D.F. Shriver, J. Am. Chem. Soc., 102 (1980) 1456.
[26] K. Whitmire and D.F. Shriver, J. Am. Chem. Soc., 103 (1981) 6754.
[27] M.A. Drezdon and D.F. Shriver, J. Mol. Catal., 21 (1983) 81.
[28] D.M.P. Mingos and D.J. Wales, Introduction to Cluster Chemistry, Prentice-Hall, Englewood Cliffs, NJ, 1990.
[29] M. Blohm and W.L. Gladfelter, Organometallics, 5 (1986) 1049.
[30] T. Dutton, B.F.G. Johnson, J. Lewis, S.M. Owen and P.R. Raithby, J. Chem. Soc., Chem. Commun., (1988) 1423.
[31] F.-E. Hong, D.A. McCarthy, J.P. White III, C.E. Cottrell and S.G. Shore, Inorg. Chem., 29 (1990) 2874.
[32] A.K. Chipperfield, C.E. Housecroft and A.L. Rheingold, Organometallics, 9 (1990) 681.
[33] N.N. Greenwood, R.V. Parish and P. Thornton, Q. Rev. Chem. Soc., 20 (1966) 441.
[34] C.E. Housecroft, D.M. Matthews, A.L. Rheingold and X. Song, J. Chem. Soc., Chem. Commun., (1992) 842.

[35] C.E. Housecroft, D.M. Matthews, A. Waller, A.J. Edwards and A.L. Rheingold, J. Chem. Soc., Dalton Trans., (1993) 3059.
[36] T.P. Fehlner, M.M. Amini, M.V. Zeller, W.F. Stickle, O.A. Pringle, G.J. Long and F.P. Fehlner, Mater. Res. Soc. Symp. Proc., 131 (1989) 413.
[37] J.P. White III, H. Deng and S.G. Shore, Inorg. Chem., 30 (1991) 2337.
[38] J. Mason, J. Am. Chem. Soc., 113 (1991) 6056.
[39] M.J. Duer and D.J. Wales, Polyhedron, 10 (1991) 1749.
[40] R. Khattar, T.P. Fehlner and P.T. Czech, New J. Chem., 15 (1991) 705.
[41] N.P. Rath and T.P. Fehlner, J. Am. Chem. Soc., 110 (1988) 5345.
[42] C.E. Housecroft and co-workers, unpublished observations.
[43] T.P. Fehlner, P.T. Czech and R.F. Fenske, Inorg. Chem., 29 (1990) 3103.
[44] K.S. Wong, W.R. Scheidt and T.P. Fehlner, J. Am. Chem. Soc., 104 (1982) 1111.
[45] S.M. Draper, C.E. Housecroft, A.K. Keep, D.M. Matthews, X. Song and A.L. Rheingold, J. Organomet. Chem., 423 (1992) 241.
[46] J.-H. Chung, D. Knoeppel, D. McCarthy, A. Columbie and S.G. Shore, Inorg. Chem., 32 (1993) 3391.
[47] F.-E. Hong, T.J. Coffy, D. McCarthy and S.G. Shore, Inorg. Chem., 28 (1989) 3284.
[48] A.K. Chipperfield, C.E. Housecroft and P.R. Raithby, Organometallics, 9 (1990) 479.
[49] C.R. Eady, B.F.G. Johnson and J. Lewis, J. Chem. Soc., Dalton Trans., (1977) 477.
[50] G.B. Jacobsen, E.L. Andersen, C.E. Housecroft, F.-E. Hong, M.L. Buhl, G.J. Long and T.P. Fehlner, Inorg. Chem., 26 (1987) 4040.
[51] C.E. Housecroft, M.L. Buhl, G.J. Long and T.P. Fehlner, J. Am. Chem. Soc., 109 (1987) 3323.
[52] X. Meng, A.K. Bandyopadhyay and T.P. Fehlner, J. Organomet. Chem., 394 (1990) 15.
[53] C.E. Housecroft and T.P. Fehlner, Organometallics, 5 (1986) 379.
[54] C.E. Housecroft, D.M. Matthews, A.L. Rheingold and X. Song, J. Chem. Soc., Dalton Trans., (1992) 2855.
[55] D.F. Shriver, H.D. Kaesz and R.D. Adams (eds.), Transition Metal Cluster Chemistry, VCH, New York, 1990.
[56] J.R. Galsworthy, C.E. Housecroft, D.M. Matthews, R. Ostrander and A.L. Rheingold, J. Chem. Soc., Dalton Trans., (1994) 69.
[57] J.R. Galsworthy, C.E. Housecroft and A.L. Rheingold, Organometallics., (1993) 4167.
[58] J.R. Galsworthy, C.E. Housecroft and A.L. Rheingold, J. Chem. Soc., Dalton Trans., (1994), 2359.
[59] D.-Y. Jan, D.P. Workman, L.-Y. Hsu, J.A. Krause and S.G. Shore, Inorg. Chem., 31 (1992) 5123, and references cited therein.
[60] T.P. Fehlner, C.E. Housecroft, W.R. Scheidt and K.S. Wong, Organometallics, 2 (1983) 825.
[61] K. Wade, Adv. Inorg. Chem. Radiochem., 18 (1976) 1.
[62] D.M.P. Mingos, Nature, 236 (1972) 99.
[63] J.W. Lauher, J. Am. Chem. Soc., 100 (1978) 5305.
[64] C.E. Housecroft and T.P. Fehlner, Organometallics, 5 (1986) 1279.
[65] N.P. Rath and T.P. Fehlner, J. Am. Chem. Soc., 109 (1987) 5273.
[66] T.P. Fehlner, Comments Inorg. Chem., 7 (1988) 326.
[67] T.P. Fehlner, Polyhedron, 9 (1990) 1955.
[68] S.M. Draper, Ph.D. Thesis, University of Cambridge, 1991.
[69] C.E. Housecroft and J.S. Humphrey, unpublished observations.
[70] A.K. Chipperfield, B.S. Haggerty, C.E. Housecroft and A.L. Rheingold, J. Chem. Soc., Chem. Commun., (1990) 1174.
[71] C.E. Housecroft, J.S. Humphrey, A.K. Keep, D.M. Matthews, N.J. Seed, B.S. Haggerty and A.L. Rheingold, Organometallics, 11 (1992) 4048.
[72] S.M. Draper, C.E. Housecroft, A.K. Keep, D.M. Matthews, B.S. Haggerty and A.L. Rheingold, J. Organomet. Chem., 410 (1991) C44.
[73] J.R. Galsworthy, C.E. Housecroft, J.S. Humphrey, X. Song, A.J. Edwards and A.L. Rheingold, J. Chem. Soc., Dalton Trans., (1994), 3273.
[74] L.E. Crascall, B.H.S. Thimmappa, A.L. Rheingold, R. Ostrander and T.P. Fehlner, Organometallics, 13 (1994) 2153.

[75] I.D. Salter, Adv. Organomet. Chem., 29 (1989) 249.
[76] (a) C.E. Housecroft and A.L. Rheingold, J. Am. Chem. Soc., 108 (1986) 6420.
(b) C.E. Housecroft and A.L. Rheingold, Organometallics, 6 (1987) 1332.
[77] C.E. Housecroft, M.S. Shongwe, A.L. Rheingold and P. Zanello, J. Organomet. Chem., 408 (1991) 7.
[78] K.S. Harpp and C.E. Housecroft, J. Organomet. Chem., 340 (1988) 389.
[79] S.M. Draper, C.E. Housecroft, J.E. Rees, M.S. Shongwe, B.S. Haggerty and A.L. Rheingold, Organometallics, 11 (1992) 2356.
[80] C.E. Housecroft, M.S. Shongwe and A.L. Rheingold, Organometallics, 7 (1988) 1332.
[81] C.E. Housecroft, M.S. Shongwe and A.L. Rheingold, Organometallics, 8 (1989) 2651.
[82] K.S. Harpp, C.E. Housecroft, M.S. Shongwe and A.L. Rheingold, J. Chem. Soc., Chem. Commun., (1988) 965.
[83] S.M. Draper, C.E. Housecroft and A.L. Rheingold, J. Organomet. Chem., 435 (1992) 9.
[84] D.M. Matthews, Ph.D. Thesis, University of Cambridge, 1992.
[85] C.E. Housecroft, D.M. Matthews and A.L. Rheingold, Organometallics, 11 (1992) 2959.
[86] B.F.G. Johnson, J. Lewis, W.J.H. Nelson, J.N. Nicholls, J. Puga, P.R. Raithby, M.J. Rosales, M. Schröder and M.D. Vargas, J. Chem. Soc., Dalton Trans., (1983) 2447.
[87] B.F.G. Johnson, J. Lewis, J.N. Nicholls, J. Puga, P.R. Raithby, M.J. Rosales, M. McPartlin and W. Clegg, J. Chem. Soc., Dalton Trans., (1983) 277.
[88] C-S. Jun, T.P. Fehlner and A.L. Rheingold, J. Am. Chem. Soc., 115 (1993) 4393.
[89] G. Schmid, V. Bätzel, G. Etzrodt and R. Pfeil, J. Organomet. Chem., 86 (1975) 257.
[90] A. Bandyopadhyay, M. Shang, C.S. Jun and T.P. Fehlner, Inorg. Chem., 33 (1994) 3677.
[91] R. Khattar, J. Puga, T.P. Fehlner and A.L. Rheingold, J. Am. Chem. Soc., 111 (1989) 1877.
[92] A.K. Bandyopadhyay, R. Khattar and T.P. Fehlner, Inorg. Chem., 28 (1989) 4437.
[93] A.K. Bandyopadhyay, R. Khattar, J. Puga, T.P. Fehlner and A.L. Rheingold, Inorg. Chem., 31 (1992) 465.
[94] A.D. Hattersley, Ph.D. Thesis, University of Cambridge, 1993.
[95] J.R. Galsworthy, A.D. Hattersley, C.E. Housecroft, A.L. Rheingold and A. Waller, J. Chem. Soc., Dalton Trans., (1995), in press.
[96] E. Andersen and T.P. Fehlner, J. Am. Chem. Soc., 100 (1978) 4606.
[97] C.-S. Jun, X. Meng, K.J. Haller and T.P. Fehlner, J. Am. Chem. Soc., 113 (1991) 3603.
[98] C.-S. Jun, D.R. Powell, K.J. Haller and T.P. Fehlner, Inorg. Chem., 32 (1993) 5071.
[99] C.E. Housecroft, A.L. Rheingold and M.S. Shongwe, J. Chem. Soc., Chem. Commun., (1988) 1630.
[100] S.M. Draper, A.D. Hattersley, C.E. Housecroft and A.L. Rheingold, J. Chem. Soc., Chem. Commun., (1992) 1365.
[101] F.H. Allen, J.E. Davies, J.J. Galloy, O. Johnson, O. Kennard, C.F. Macrae, E.M. Mitchell, G.F. Mitchell, J.M. Smith and D.G. Watson, J. Chem. Inf. Comput. Sci., 31 (1991) 187.